



32 vegetation types located in arid regions showed the strongest response to drought.
33 Importantly, this study stresses that the time scale at which drought is assessed is a
34 dominant factor in understanding the different responses of vegetation activity to
35 drought.

36 **Key-words:** Drought, NDVI, Vegetation activity, Climatic change, Spain.

37

38 **1. Introduction**

39 Drought is one of the major hydroclimatic hazards impacting land surface fluxes
40 (Baldocchi et al., 2004; Fischer et al., 2007; Hirschi et al., 2011), vegetation respiration
41 (Ciais et al., 2005), net primary production (Reichstein et al., 2007; Zhao and Running,
42 2010), primary and secondary forest growth (Allen et al., 2015), and crop yield (Lobell
43 et al., 2015; Asseng et al., 2015). Recently, numerous studies suggested an accelerated
44 impact of drought on vegetation activity and forest mortality under different
45 environmental conditions (Allen et al., 2010, 2015; Breshears et al., 2005) with a
46 reduction in vegetation activity and higher rates of tree decay (e.g. Carnicer et al., 2011;
47 Restaino et al., 2016). Nevertheless, a comprehensive assessment of the impacts of
48 drought on vegetation activity is a challenging task. This is particularly because data on
49 forest conditions and growth are partial, spatially sparse, and restricted to a small
50 number of sampled forests (Grissino-Mayer and Fritts, 1997). Furthermore, the
51 temporal resolution of forest data is insufficient to provide deep insights into the
52 impacts of drought on vegetation activity [e.g. the official forest inventories (Jenkins et
53 al., 2003)]. In addition to these challenges, the spatial and temporal data on crops are
54 often limited, as they are mostly aggregated to administrative levels and provided at the
55 annual scale, with minor information on vegetation activity across the different periods
56 of the year (e.g. <http://faostat.fao.org>; <https://quickstats.nass.usda.gov/#AF9A0104-19EF-3BFE-90D2-C67700892F3E>;
57 <https://quickstats.nass.usda.gov/#AF9A0104-19EF-3BFE-90D2-C67700892F3E>; last access on 1st October 2018). To handle these



58 limitations, numerous studies have alternatively employed the available remotely sensed
59 data to assess the impacts of drought on vegetation activity (e.g. Ji and Peters, 2003;
60 Wan et al., 2004; Rhee et al., 2010; Zhao et al., 2017).

61 Several space-based products allow for quantifying vegetation conditions, given that
62 both health and dry vegetation biomass respond dissimilarly to the electromagnetic
63 radiation received in the visible and near-infrared parts of the vegetation spectrum
64 (Knipling, 1970). As such, with the available spectral information recorded by sensors
65 on board of satellite platforms, it is possible to calculate vegetation indices and
66 accordingly assess vegetation activity (Tucker, 1979). In this context, several studies
67 have already employed vegetation indices not only to develop drought-related metrics
68 (e.g. Kogan, 1997; Mu et al., 2013), but to determine the impacts of drought on
69 vegetation conditions as well (García et al., 2010; Vicente-Serrano et al., 2013; Zhang et
70 al., 2017). An inspection of these studies reveals that drought impacts can be
71 characterized using vegetation indices, albeit with a different response of vegetation
72 dynamics as a function of a wide-range of factors, including –among others– vegetation
73 type, bioclimatic conditions, and drought severity (Bhuiyan et al., 2006; Vicente-
74 Serrano, 2007; Quiring and Ganesh, 2010; Ivits et al., 2014).

75 Given high interannual variability of precipitation, combined with the prevailing semi-
76 arid conditions across vast areas of the territory, Spain has suffered from frequent,
77 intense and severe drought episodes during the past decades (Vicente-Serrano, 2006).
78 Nonetheless, in the era of temperature rise, the observed increase in atmospheric
79 evaporative demand (AED) during the last decades has accelerated the severity of
80 droughts (Vicente-Serrano et al., 2014c), in comparison to the severity caused only by
81 precipitation deficits (Vicente-Serrano et al., 2014a; González-Hidalgo et al., 2018).
82 Over Spain, the hydrological and socioeconomic impacts of droughts are well-



83 documented. Hydrologically, droughts are often associated with a decrease in
84 streamflow and reservoir storages (Lorenzo-Lacruz et al., 2010; Lorenzo-Lacruz et al.,
85 2013). The impacts of drought can extend further to crops, leading to crop failure due to
86 deficit in irrigation water (Iglesias et al., 2003), and even in arable non-irrigated lands
87 (Austin et al., 1998; Páscoa et al., 2017). Over Spain, numerous investigations also
88 highlighted the adverse impacts of drought on forest growth (e.g. Camarero et al., 2015;
89 Gazol et al., 2018; Peña-Gallardo et al., 2018) and forest fires (Hill et al., 2008; Lasanta
90 et al., 2017; Pausas, 2004; Pausas and Fernández-Muñoz, 2012).

91 Albeit with these adverse drought-driven impacts, there is a lack of comprehensive
92 studies that assess the impacts of drought on vegetation activity over the entire Spanish
93 territory, with a satisfactorily temporal coverage. While numerous studies employed
94 remotely sensed imagery and vegetation indices to analyze spatial and temporal
95 variability and trends in vegetation activity over Spain (e.g. del Barrio et al., 2010;
96 Julien et al., 2011; Stellmes et al., 2013), few attempts have been made to link the
97 temporal dynamics of satellite-derived vegetation activity with climate variability and
98 drought evolution (e.g. Vicente-Serrano et al., 2006; Udelhoven et al., 2009; Gouveia et
99 al., 2012; Mühlbauer et al., 2016). An example is González-Alonso and Casanova
100 (1997) who analyzed the spatial distribution of droughts in 1994 and 1995 over Spain,
101 concluding that the most affected areas are semiarid regions. In their comparison of the
102 MODIS Normalized Difference Vegetation Index (NDVI) data and the Standardized
103 Precipitation Index (SPI) over Spain, García-Haro et al. (2014) indicated that the
104 response of vegetation dynamics to climate variability is highly variable, according to
105 the regional climate conditions, vegetation community, and growth stages. A similar
106 finding was also confirmed by Vicente-Serrano (2007) and Contreras and Hunink
107 (2015) in their assessment of the response of NDVI to drought in semiarid regions of



108 northeast and southeast Spain, respectively. Albeit with these comprehensive efforts, a
109 detailed spatial assessment of the links between droughts and vegetation activity, which
110 covers a long time period (decades), is highly desired for Spain to explore the
111 differences in the response of vegetation activity to drought under different
112 environments with various land cover and vegetation types.

113 The overriding objectives of this study are: i) to determine the possible differences in
114 the response of vegetation activity to drought over Spain, as a function of the different
115 land cover types and climatic conditions; and ii) to explore the drought time scales at
116 which vegetation activity highly responds to drought severity. An innovate aspect of
117 this study is that it provides –for the first time– a comprehensive assessment of the
118 response of vegetation activity to drought using a multidecadal (1981-2015) high spatial
119 resolution (1.1 km) NDVI dataset over the study region.

120

121 **2. Data and methods**

122 **2.1. Datasets**

123 *2.1.1. NDVI data*

124 Globally, there are several NDVI datasets, which have been widely used to analyze
125 NDVI variability and trends (e.g. Slayback et al., 2003; Herrmann et al., 2005;
126 Anyamba and Tucker, 2005) and to assess the links between NDVI and climate
127 variability and drought (e.g. Dardel et al., 2014; Vicente-Serrano et al., 2015; Gouveia
128 et al., 2016). Amongst these global datasets, the most widely used are those derived
129 from the Advanced Very High Resolution Radiometer (AVHRR) sensor on board of the
130 NOAA satellites and those retrieved from the Moderate Resolution Imaging
131 Spectroradiometer (MODIS) data. Both products have been widely employed to
132 evaluate the possible influence of drought on vegetation dynamics in different regions



133 worldwide (e.g. Tucker et al., 2005; Gu et al., 2007; Sona et al., 2012; Pinzon and
134 Tucker, 2014; Ma et al., 2015). While the Global Inventory Modeling and Mapping
135 Studies (GIMMS) dataset from NOAA-AVHRR is available at a semi-monthly
136 temporal resolution for the period from 1981 onwards (Tucker et al., 2005; Pinzon and
137 Tucker, 2014), its spatial resolution is quite low (64 km²), which makes it difficult to
138 capture the high spatial variability of vegetation cover over Spain. On the other hand,
139 the NDVI dataset derived from MODIS dates back only to 2001 (Huete et al., 2002),
140 which is insufficient to give insights into the long-term response of vegetation activity
141 to drought. To overcome these spatial and temporal limitations, our decision was made
142 to employ a recently developed high-resolution spatial NDVI dataset (Sp_1Km_NDVI),
143 which is available at grid interval of 1.1 km, spanning the period from 1981 onwards. In
144 accordance with GIMMS dataset, Sp_1Km_NDVI is available at a semi-monthly
145 temporal resolution. This dataset has already been validated (Vicente-Serrano et al.,
146 2018), showing high performance in comparison to other available NDVI datasets. As
147 such, it can be used -with confidence- to provide a multidecadal assessment of NDVI
148 variability at high-spatial resolution, especially in areas of highly variable vegetation.
149 Herein, it is noteworthy indicating that the data from the Sp_1Km_NDVI dataset was
150 standardized (sNDVI), so that each series has an average equal to zero and a standard
151 deviation equal to one. This procedure is motivated by the strong seasonality and spatial
152 differences of vegetation activity over Spain. Following this procedure, the magnitudes
153 of all NDVI time series are comparable over space and time. To accomplish this task,
154 the data were fitted to a log-logistic distribution, which shows better skill in
155 standardizing environmental variables, in comparison to other statistical distributions
156 (Vicente-Serrano and Beguería, 2016).



157 In our attempt to limit the possible impact of changes in land cover on the dependency
158 between drought and vegetation cover, we assumed that strong changes in NDVI can be
159 seen as an indicator of changes in land cover. As such, those pixels with strong changes
160 in NDVI during the study period were excluded from the analysis. These pixels were
161 defined after an exploratory analysis in which we tested different thresholds. In specific,
162 we excluded those pixels, which exhibited a decrease in the annual NDVI higher than
163 0.05 units or an increase higher than 0.15 units between 1981 and 2015. The spatial
164 distribution (not shown here) of these pixels concurs well with the areas identified in
165 earlier studies over Spain (e.g. Lasanta and Vicente-Serrano, 2012; Vicente-Serrano et
166 al., 2018). Furthermore, to avoid the possible influence of spatial autocorrelation, which
167 can occur in areas with dominant positive changes in NDVI due to excessive rural
168 exodus and natural revegetation processes (Hill et al., 2008; Vicente-Serrano et al.,
169 2018), we detrended the standardized NDVI series by means of a linear model. We then
170 add the residuals of the linear trend to the average of NDVI magnitude over the study
171 period. A similar approach has been adopted in several environmental studies (Olsen et
172 al., 2013; Xulu et al., 2018; Zhang et al., 2016).

173

174 ***2.1.2. Drought dataset***

175 Due to its complicated physiological strategies to cope with water stress, vegetation can
176 show specific and even individual resistance and vulnerability to drought (Chaves et al.,
177 2003; Gazol et al., 2017; Gazol et al., 2018). As such, it is quite difficult to directly
178 assess the impacts of drought on vegetation activity and forest growth. Alternatively,
179 drought indices can be an appropriate tool to make this assessment, particularly with
180 their calculation at multiple time scales. These time scales summarize the accumulated
181 climatic conditions over different periods, which make drought indices closely related



182 to impact studies. Overall, to calculate drought indices, we employed data for a set of
183 meteorological variables (i.e. precipitation, maximum and minimum air temperature,
184 relative humidity, sunshine duration, and wind speed) from a recently developed
185 gridded climatic dataset (Vicente-Serrano et al., 2017). This gridded dataset was
186 developed using a dense network of quality-controlled and homogenized meteorological
187 records. Data are available for the whole Spanish territory at a spatial resolution of 1.1
188 km, which is consistent with the resolution of the NDVI dataset (section 2.1.1). Based
189 on this gridded dataset, we computed the atmospheric evaporative demand (AED),
190 reference evapotranspiration (ET_o), and the Standardized Precipitation
191 Evapotranspiration Index (SPEI). ET_o was calculated using the physically based FAO-
192 56 Penman-Monteith equation (Allen et al., 1998). On the other hand, the SPEI was
193 computed using precipitation and AED data (Vicente-Serrano et al., 2010). The SPEI is
194 one of the most widely used drought indices and has thus been employed to quantify
195 drought in a number of agricultural (e.g. Peña-Gallardo et al., 2018b), environmental
196 (e.g. Vicente-Serrano et al., 2012; Bachmair et al., 2018), and socioeconomic
197 applications (e.g. Bachmair et al., 2015; Stagge et al., 2015). The SPEI is advantageous
198 compared to the Palmer Drought Severity Index (PDSI), as it is calculated at different
199 time scales. In comparison to the Standardized Precipitation Index (SPI) (McKee et al.,
200 1993), the SPEI does not account only for precipitation, but it also considers the
201 contribution of AED in drought evolution.

202 In this work, the SPEI was calculated for the common 1- to 24-month time scales. The
203 preference to use various time scales is motivated by our intention to characterize the
204 response of different hydrological and environmental systems to drought. It is well-
205 recognized that natural systems can show different responses to the time scales of
206 drought (Vicente-Serrano et al., 2011, 2013). The time scale refers to the period in



207 which antecedent climate conditions are accumulated and it allows to adapt the drought
208 index to the drought impacts since different hydrological and environmental systems
209 show different responses sensitivities to the time scales of climate variability. This has
210 been shown for hydrological systems (López-Moreno et al., 2013; Barker et al., 2016),
211 but also ecological and agricultural systems show strong differences in the response to
212 different time scales of climatic droughts (Pasho et al., 2011; Peña-Gallardo et al.,
213 2018b) given different biophysical conditions, but also the different strategies of
214 vegetation types to cope with water stress (Chaves et al., 2003; McDowell et al., 2008),
215 which are strongly variable in complex Mediterranean ecosystems. For instance,
216 drought indices can be calculated on flexible time scales since it is not known a priori
217 the most suitable period at which the NDVI is responding. Herein, we also detrended
218 and standardized the semi-monthly SPEI data to be comparable with the de-trended
219 sNDVI.

220 Finally, we used the CORINE Land Cover for 2000 ([https://land.copernicus.eu/pan-](https://land.copernicus.eu/pan-european/corine-land-cover)
221 [european/corine-land-cover](https://land.copernicus.eu/pan-european/corine-land-cover)) to determine how land cover can impact the response of
222 NDVI to drought severity. This map is representative of the main classes of land cover
223 in the study domain over the period of investigation.

224

225 *2.2. Statistical analysis*

226 We used the Pearson's r correlation coefficient to assess the relationship between the
227 interannual variability of the sNDVI and SPEI. This association was evaluated
228 independently for each semi-monthly period of the year. In specific, we calculated the
229 correlation between the sNDVI for each semi-monthly period and SPEI recorded in the
230 same period, at time-scales between 1- and 48-semi-months. Significant correlations
231 were set at $p < 0.05$. Importantly, as the data of the sNDVI and SPEI were de-trended,



232 the possible impact of serial correlation on the correlation between sNDVI and SPEI is
233 minimized, with no spurious correlation effects that can be expected from the co-
234 occurrence of the trends. Similarly, as the data were analyzed for each semi-monthly
235 period independently, our results are free from any seasonality effect.

236 Based on the correlation coefficients between the sNDVI and SPEI in the study domain,
237 we determined the semi-monthly period of the year and the SPEI time scale at which the
238 maximum correlation is found. This information was then used to determine the spatial
239 and seasonal variations according to the different land cover categories. Finally, the
240 average climate conditions over the study domain, including aridity (precipitation minus
241 AED) and average temperature, were related to the time-scales at which the maximum
242 correlation between the sNDVI and SPEI was found.

243

244 **3. Results**

245 ***3.1. General influence of drought on the sNDVI***

246 Figure 1 shows an example of the spatial distribution of the Pearson's r correlation
247 coefficients calculated between the sNDVI and the SPEI at the time-scales of 1-, 3-, 6-
248 and 12-months (2-, 6-, 12- and 24-semi-monthly periods). Results are shown only for
249 the second semi-monthly period of each month between April and July. The differential
250 response of the NDVI to the different time scales of the SPEI is illustrated. As depicted,
251 the 6-month time scale was more relevant to vegetation activity in large areas of
252 Southwestern and Southeastern Spain during the second half of April. On the other
253 hand, vegetation activity was more determined by the 12-month SPEI across the Ebro
254 basin in northeastern Spain. This stresses the need of considering different drought time
255 scales to know the climate cumulative period that mostly affects vegetation activity. The
256 6-month and 12-month SPEI produced similar results during the second period of May,



257 while the 12-month time scale is more related to vegetation activity in June and July.
258 The density plots (supplementary Figures 1 to 4) summarize the magnitude of
259 correlations between the SPEI and sNDVI for Spain, as a function of the semi-monthly
260 period as well as the SPEI time scale. It can be seen that correlations tend to be higher
261 during the warm season (May to August), and at time scales between 6 and 24 months.
262 Figure 2 summarizes the maximum correlation between the sNDVI and the SPEI,
263 providing insights into the differential response of the NDVI to drought. It can be noted
264 that there are clear seasonal and spatial differences in the response of sNDVI to the
265 SPEI. The sNDVI is more related to the SPEI during the warm season (MJJA). In
266 contrast, the response of the sNDVI to drought is less pronounced from September to
267 April, albeit with some exceptions. One example is the response of vegetation to
268 drought alongside the southeastern Mediterranean coastland, where the correlation
269 between sNDVI and SPEI is almost high all the year around. Table 1 summarizes the
270 percentage of the total area exhibiting significant or non-significant correlations over
271 Spain during the different semi-monthly periods. Positive (lower sNDVI with drought)
272 and statistically significant correlations are dominant across the entire territory, but with
273 a seasonal component. In particular, a higher percentage of the territory shows positive
274 and significant correlations during the warm season (MJJA). From mid of May to mid
275 of September, more than 80% of the study domain show positive and significant
276 correlations between the sNDVI and the SPEI. A similar finding is also found between
277 the mid of June and the beginning of August. Figure 3 summarizes the average
278 correlations between the SPEI and sNDVI. As illustrated, there is a gradual increase in
279 the response of the sNDVI to the SPEI from the beginning of May to the end of July,
280 when the maximum average correlation is recorded. In contrast, the correlations
281 between the SPEI and sNDVI decrease progressively from August to December.



282 The response of the sNDVI to different times scales of the SPEI and seasons is quite
283 complex. Figure 4 shows the spatial distribution of the SPEI time scale at which the
284 maximum correlation was found for each one of the 24 semi-monthly periods of the
285 year. It can be noted that there are considerable seasonal and spatial differences.
286 Nonetheless, these differences are masked with the estimated average values of the
287 SPEI time scale recorded for the semi-monthly periods (Figure 5) which are less
288 variable (oscillating between 18 and 22 semi-monthly periods -9 to 11 months-)
289 throughout the year. In general, the areas and periods with higher correlations are
290 recorded at the time scales between 7 and 24 semi-months (3-12 months). This pattern
291 is mostly recorded in the period between May and July (Supplementary Figure 5), in
292 which the sNDVI variability is more sensitive to drought. Nevertheless, there are no
293 general spatial patterns in the response of the NDVI to SPEI, indicating that there is a
294 dominance of the maximum correlations associated with a certain SPEI time scale
295 (Supplementary Figure 6). Interestingly, this , this pattern is not driven by the presence
296 of different land cover types, given that the correlation coefficients between the sNDVI
297 and SPEI are quite similar, irrespective of the land cover type (Supplementary Figures 7
298 to 17).

299

300 ***3.2. Land cover differences***

301 There are differences in the magnitude and seasonality of the Pearson's r correlation
302 coefficients among all land cover types. Figure 6 shows the average and standard error
303 of the mean of the maximum Pearson's r coefficients between the sNDVI and SPEI for
304 the different land cover types and the 24 semi-monthly periods. The magnitudes of
305 correlation vary considerably, as a function of land cover type, as well as the period of
306 the year in which the highest correlations are recorded. The non-irrigated arable lands



307 show a peak of significant correlation between April and June. However, this
308 correlation decreases towards the end of the year. The majority of the surface dominated
309 by this land cover shows positive and significant correlations between May and
310 September (Supplementary Table 1), with percentages almost close to 100%. On the
311 contrary, irrigated lands do not show such a strong response to drought during the warm
312 season. Even with the presence of a seasonal pattern, it is less pronounced than the one
313 observed for non-irrigated arable lands. Overall, irrigated areas are characterized by
314 positive and significant correlations between sNDVI and SPEI during summertime
315 (Supplementary Table 2). Similarly, vineyards show a clear seasonal pattern, albeit with
316 a peak of maximum correlations during the late summer (July-August) and early
317 autumn (September-October) (Supplementary Table 3). On the other hand, olive groves
318 show of the highest correlation between the sNDVI and SPEI during the second half of
319 May and in October, suggesting a quasi bi-modal response of the NDVI to drought.
320 This pattern is also revealed in the percentage of the surface area with significant
321 correlations (Supplementary Table 4). In the same context, the areas of natural
322 vegetation exhibit their maximum correlation between the sNDVI and SPEI during
323 summer months. The highest correlations are found in July and August for the forest
324 types, compared to earlier June for the natural grasslands and the areas of sclerophyllous
325 vegetation. On the other hand, the mixed forests tend to show lower correlations than
326 broad-leaved and coniferous forests. A quick inspection of all these types of land cover
327 indicates that the correlations between the sNDVI and SPEI are generally positive and
328 significant during summer months (Supplementary Tables 5 to 11).

329 Large differences across vegetation types were found for the SPEI time scales at which
330 maximum correlations between sNDVI and the SPEI are found (Figure 7). For example,
331 for non-irrigated arable lands, the maximum correlation between SPEI and sNDVI is



332 found for time scales between 11 and 21 semi-monthly periods. This indicates that
333 crops in May-June (the period in which higher correlations are recorded) respond
334 mostly to the climate conditions recorded between June and December of the preceding
335 year. Irrigated lands show a clear seasonal pattern, as maximum correlations are
336 recorded at time scales between 12 and 18 semi-monthly periods (i.e. 6 to 9 months),
337 mainly between November and May. On the other hand, the maximum correlations
338 between sNDVI and SPEI during summer are found for time scales between 25 and 28
339 semi-monthly periods. Similar to irrigated lands, vineyards show a strong seasonality,
340 responding to longer time-scales at the end of summertime. In contrast, natural
341 vegetation areas show less seasonality to SPEI time scales, which mostly impact the
342 interannual variability of sNDVI. The SPEI time scales, at which the maximum
343 correlation is found between sNDVI and SPEI, vary from 20 semi-monthly periods
344 during the warm season (MJJAS) to 30 semi-monthly periods during the cold season
345 (ONDJFMA). This finding is evident for all forest types and areas of sclerophyllous
346 vegetation and mixed wood-scrub. The only exception corresponds to natural
347 grasslands, which show a response to shorter SPEI time scales (i.e. 20 semi-monthly
348 periods in winter and 15 in spring and early summer).

349

350 ***3.3. Influence of average climatic conditions***

351 In addition to the impact of the time scale at which drought is quantified, the response
352 of vegetation activity to drought can also be closely related to the prevailing climatic
353 conditions. Figure 8 summarizes the spatial correlation between aridity (P-AED) and
354 the maximum correlation between the sNDVI and SPEI. For most of the semi-monthly
355 periods of the year aridity is negatively correlated with the maximum correlation
356 between sNDVI and SPEI, indicating that vegetation activity in arid sites is more



357 responsive to drought variability. This correlation is more pronounced for the period
358 between December and June. In contrast, this negative association becomes weaker and
359 statistically non-significant during warmer months (e.g. July and August). Figure 9
360 illustrates the spatial correlation between mean air temperature and the maximum
361 correlation between the sNDVI and SPEI. Results demonstrate similar results to those
362 found for aridity, with a general positive and significant correlation from March to June,
363 followed by a non-significant and weak correlation during summer months.

364 Nonetheless, these general patterns vary largely as a function of land cover type
365 (Supplementary Figures 18 to 28). For example, in non-irrigated arable lands, there is
366 strong negative correlation between aridity and the sNDVI/SPEI maximum correlation
367 from March to May: a period that witnesses the peak of vegetation activity in this land
368 cover type. This also coincides with the period of the highest average correlations
369 between the sNDVI and SPEI. Taken together, this demonstrates that non-irrigated
370 arable lands located in the most arid areas are more sensitive to drought variability than
371 those located in humid regions. As opposed to non-irrigated arable lands, the
372 correlations with aridity are found statistically non-significant in all periods of the year
373 for irrigated lands, vineyards and olive groves. Nevertheless, for the different natural
374 vegetation categories, the correlations are negative and statistically significant during
375 large periods. The mixed agricultural/natural vegetation areas show a significant
376 correlation between October and July, with stronger association at the beginning of
377 summer season. Broadleaved and coniferous forests, scrubs, and pasture lands also
378 show a negative relationship between the spatial patterns of the sNDVI/SPEI
379 correlations and aridity.

380 As depicted in Figure 9, the relationship between the sNDVI/SPEI correlation and air
381 temperature shows that the response of vegetation activity to drought is modulated by



382 air temperature during springtime. This implies that warmer areas are those in which the
383 sNDVI is more controlled by drought. A contradictory pattern is found during warmer
384 months, in which the role of air temperature in modulating the impact of drought on
385 vegetation activity is minimized. The relationships between air temperature and the
386 NDVI-SPEI correlation vary among the different land cover types (Supplementary
387 Figures 29 to 39). For example, in non-irrigated arable lands, the positive and
388 statistically significant correlation is found in the period from March to April, indicating
389 that the response of the sNDVI to SPEI tends to coincide spatially with areas of warmer
390 conditions. As observed for aridity, the relationship between the sNDVI and SPEI in
391 irrigated lands is less associated with the spatial patterns of air temperature. A similar
392 pattern is recorded for vineyards and olive groves. Nevertheless, the areas of natural
393 vegetation show a clear relationship between air temperature and the sNDVI/SPEI
394 correlations. In the mixed agriculture and natural vegetation areas, we found a
395 statistically significant positive association between the sNDVI and SPEI from October
396 to May. On the contrary, this association is less evident during summer months. This
397 general association during springtime, combined with the lack of association during
398 summertime, can also be seen for other natural vegetation types such as broad-leaved
399 and coniferous forests, natural grasslands, sclerophyllous vegetation and mixed wood-
400 scrubs.

401 We also analyzed the dependency between climatic conditions (i.e. aridity and air
402 temperature) and the SPEI time scale(s) at which the maximum correlation between the
403 sNDVI and SPEI is recorded. Figure 10 shows the values of aridity corresponding to
404 SPEI time scales at which the maximum correlation between the sNDVI and SPEI is
405 found for each semi-monthly period. The different box-plots indicate complex patterns,
406 which are quite difficult to interpret. Overall, less arid areas show stronger correlations



407 at longer time-scales (25-42 semi-monthly periods) during springtime. In the same
408 context, the regions with maximum correlations at short time scales (1-6 months) tend
409 to be located in less arid regions that record their maximum correlations at time scales
410 between 7 and 24 semi-monthly periods. This suggests that the most arid areas mostly
411 respond to the SPEI time scales between 6 and 12 months, compared to short (1-3
412 months) or long (> 12 months) SPEI time-scales in more humid regions. In contrast,
413 during summer season, the interannual variability of the sNDVI in the arid areas is
414 mostly determined by the SPEI recorded at time scales higher than 6 months (12 semi-
415 monthly periods), while responding to short SPEI time scales (< 3 months) over the
416 most humid regions.

417 Again, this general pattern is highly dependent on the land cover type (Supplementary
418 Figures 40 to 50). In the non-irrigated arable lands, there are no noticeable differences
419 in aridity in response to the SPEI time scale that recorded the maximum correlation with
420 the sNDVI. A similar finding is also found irrespective of the considered semi-monthly
421 period. In the vineyards, we noted that the sNDVI responds to short SPEI time scales in
422 areas characterized by lower aridity conditions during summer months. This pattern is
423 less evident for olive groves. In contrast, we observed clear patterns for natural
424 vegetation. In particular, those areas characterized by mixed agriculture and vegetation
425 show high complexity during winter and spring, with no specific patterns in relation to
426 the SPEI time-scales with maximum correlations with the sNDVI. In contrast, we found
427 a clear pattern during warmer months (June to September), with stronger correlations at
428 shorter time scales in the most humid areas and at longer SPEI time-scales (> 12
429 months) over the most arid regions. The pattern is less pronounced in broad-leaved
430 forests, although the response to short SPEI time scales seems to be more frequent in
431 the less arid broad-leaved forests. On the other hand, in coniferous forests,



432 sclerophyllous vegetation, and the transition wood-scrub, we noted a relationship
433 between the aridity and the SPEI time-scales with maximum correlation with the
434 sNDVI during summer months. Natural grassland areas show clear seasonal differences.
435 In spring, the grasslands located in the most arid sites show higher correlation at short
436 SPEI time scales, while they exhibit similar patterns (i.e. maximum correlations at short
437 SPEI time scales under less arid conditions) to those of other natural vegetation areas
438 during summer.

439 Also, we found links between the spatial distribution of air temperature and the SPEI
440 time scales at which maximum correlation between the sNDVI and SPEI is recorded
441 (Figure 11). In early spring, short SPEI time scales dominate in warmer areas, compared
442 to long SPEI time scales in colder regions. A contradictory pattern is observed from
443 June to September, with a dominance of shorter SPEI time scales in colder areas and
444 longer SPEI time scales in warmer regions. In terms of vegetation types, natural
445 vegetation areas tend generally to reproduce similar pattern in comparison to cultivation
446 types (Supplementary Figures 51 to 61).

447 The spatial distribution of all land cover types, after excluding irrigated lands in which
448 the anthropogenic factors dominate, is illustrated in Figure 12. Mixed forests are located
449 in the most humid areas, while vineyards, olive groves, non-irrigated arable lands and
450 the sclerophyllous natural vegetation are distributed in the most arid sites. Nevertheless,
451 there is a gradient of these land cover types in terms of their response to drought, as
452 those types located under more arid conditions show a stronger response of vegetation
453 activity to drought than those located in humid environments. For example, the mixed
454 forests show lower correlations than crop types and other vegetation areas. This may
455 suggest that there is a linear relationship between climate aridity corresponding to each
456 land cover and how vegetation activity will respond to drought. This pattern is more



457 evident during the different semi-monthly periods of the year, albeit with more
458 differences during spring and autumn. In summer, these differences are much smaller
459 between land cover categories, irrespective of aridity conditions.

460 There are also differences in the average SPEI time scale at which the maximum
461 sNDVI/SPEI correlation is obtained (Figure 13). However, these differences are
462 complex, with noticeable seasonal differences in terms of the relationship between
463 climate aridity and land cover types. In spring and late autumn, land cover types located
464 in more arid conditions tend to respond to shorter SPEI time scales than those located in
465 more humid areas. This pattern can be seen in late summer and early autumn, in which
466 the most arid land cover types (e.g. vineyards and olive groves) tend to respond at
467 longer SPEI time scales, compared to forest types (mostly the mixed forests), which are
468 usually located under more humid conditions.

469

470 **4. Discussion and conclusions**

471 This study assesses the response of vegetation activity to drought in Spain using a high-
472 resolution (1.1 km) spatial NDVI dataset that dates back to 1981 (Vicente-Serrano et al.,
473 2018). Based on another high-resolution semi-monthly gridded climatic dataset, drought
474 was quantified using the Standardized Precipitation Evapotranspiration Index (SPEI) at
475 different time scales (Vicente-Serrano et al., 2017).

476 Results demonstrate that vegetation activity over large parts of Spain is closely related
477 to the interannual variability of drought. In summer more than 90% of the study domain
478 show statistically significant positive correlations between the NDVI and SPEI. A
479 similar response of the NDVI to drought is confirmed in earlier studies in different
480 semi-arid and sub-humid regions worldwide, including Northeastern Brazil (e.g.
481 Barbosa et al., 2006), the Sahel (e.g. Herrmann et al., 2005), Central Asia (e.g. Gessner



482 et al., 2013), Australia (e.g. De Keersmaecker et al., 2017) and California (e.g. Okin et
483 al., 2018). Albeit with this generalized response, our results also show noticeable spatial
484 and seasonal differences in this response. These differences can be linked to the time
485 scale at which the drought is quantified, besides the impact of other dominant climatic
486 conditions (e.g. air temperature and aridity).

487 This study stresses that the response of vegetation activity to drought is more
488 pronounced during the warm season (MJJAS), in which vast areas of the Spanish
489 territory show statistically significant positive correlation between the sNDVI and SPEI.

490 This seasonal pattern can be attributed to the phenology of vegetation under different
491 land cover types. In the cold season, some areas, such as pastures and non-permanent
492 broad leaf forests, do not have any vegetation activity. Other areas, with coniferous
493 forests, shrubs and cereal crops, show a low vegetation activity. As such, irrespective of
494 the recorded drought conditions, the response of vegetation to drought would be low
495 during wintertime. This behaviour is also enhanced by the atmospheric evaporative
496 demand (AED), which is generally low in winter in Spain (Vicente-Serrano et al.,
497 2014d), with a lower water demand of vegetation and accordingly low sensitivity to soil
498 water availability. Austin et al. (1998) indicated that soil water recharge occurs mostly
499 during winter months, given the low water consumption by vegetation. However, in
500 spring, vegetation becomes more sensitive to drought due to temperature rise.
501 Accordingly, the photosynthetic activity, which determines NDVI, is highly controlled
502 by soil water availability (Myneni et al., 1995). In this study, the positive spatial
503 relationship found between air temperature and the sNDVI/SPEI correlation reinforces
504 this explanation. In spring, we found low correlations between the NDVI and SPEI,
505 even in cold areas. In contrast, warmer air temperatures during summer months
506 reinforce vegetation activity, but with some exceptions such as cereal cultivations, dry



507 pastures and shrubs, which record their maximum vegetation activity during spring.
508 This would explain why the response of vegetation activity to the SPEI is stronger
509 during summer in vast areas of Spain.
510 Also, this study suggests clear seasonal differences in the response of the NDVI to
511 drought, and in the magnitude of the correlation between the NDVI and the SPEI, as a
512 function of the dominant land cover. These differences are confirmed at different spatial
513 scales, ranging from regional and local (e.g. Ivits et al., 2014; Zhao et al., 2015;
514 Gouveia et al., 2017; Yang et al., 2018) to global (e.g. Vicente-Serrano et al., 2013),
515 Over Spain, the non-irrigated arable lands, natural grasslands and sclerophyllous
516 vegetation show an earlier response to drought, mainly in late spring and early summer.
517 This response is mainly linked to the vegetation phenology dominating in these land
518 covers, which usually reach their maximum activity in late spring to avoid dryness and
519 temperature rise during summer months. The root systems of herbaceous species are not
520 very deep, so they depend on the water storage in the most superficial soil layers
521 (Milich and Weiss, 1997), and they could not survive during the long and dry summer
522 in which the surface soil layers are mostly depleted (Martínez-Fernández and Ceballos,
523 2003). This would explain an earlier and stronger sensitivity to drought also showed in
524 other world semiarid regions (Liu et al., 2017; Yang et al., 2018; Bailing et al., 2018).
525 On the contrary, maximum correlations between the NDVI and the SPEI are recorded
526 during summer months in the forests but also in wood cultivations like vineyards and
527 olive groves. In this case, the maximum sensitivity to drought coincides with the
528 maximum air temperature and atmospheric evaporative demand (Vicente-Serrano et al.,
529 2014d). This pattern would be indicative of a different adaptation strategy of trees in
530 comparison to herbaceous vegetation, since whilst herbaceous cover would adapt to the
531 summer dryness generating the seed bank before the summer (Peco et al., 1998; Russi et



532 al., 1992), the trees and shrubs would base their adaptation on deeper root systems,
533 translating the drought sensitivity to the period of highest water demand and water
534 limitation.

535 In addition to the seasonal differences among land cover types, we have shown that in
536 Spain herbaceous crops show a higher correlation between the NDVI and the SPEI than
537 most of natural vegetation types (with the exception of the sclerophyllous vegetation).
538 This behaviour could be explained by three different factors: i) a higher adaptation of
539 natural vegetation to the characteristic climate of the region where drought is a frequent
540 phenomenon (Vicente-Serrano, 2006); ii) the deeper root systems that allow shrubs and
541 trees to obtain water from the deep soil; and iii) cultivated lands tend to be typically
542 located in drier areas than natural vegetation. Different studies showed that the
543 vegetation of dry environments tends to have a more intense response to drought than
544 sub-humid and humid vegetation (Schultz and Halpert, 1995; Abrams et al., 1990;
545 Nicholson et al., 1990; Herrmann et al., 2016). Vicente-Serrano et al. (2013) analysed
546 the sensitivity of the NDVI in the different biomes at a global scale and found a spatial
547 gradient in the sensitivity to drought, which was more important in arid and semiarid
548 regions.

549 In this study we have shown a control in the response of the NDVI to drought severity
550 by the climatic aridity. Thus, there is a significant correlation between the spatial
551 distribution of the climatic aridity and the sensitivity of the NDVI to drought, mostly in
552 spring and autumn. This could be explained because in more humid environments the
553 main limitation to vegetation growth is temperature and radiation rather than water, so
554 not all the water available would be used by vegetation reflected in a water surplus as
555 surface runoff. This characteristic would make the vegetation less sensitive to drought.
556 Drought indices are relative metrics in comparison to the long term climate with the



557 purpose of making drought severity conditions comparable between areas of very
558 different climate characteristics (Mukherjee et al., 2018). This means that in humid
559 areas the corresponding absolute precipitation can be sufficient to cover the vegetation
560 water needs although drought indices inform on below-of-the-average conditions. On
561 the contrary, in arid regions a low value of a drought index is always representative of
562 limited water availability, which would explain the closer relationship between the
563 NDVI and the SPEI.

564 Here we also explored if the general pattern observed in humid and semi-arid regions is
565 also affected by the land cover, and found that the behaviour in the non-irrigated arable
566 lands is the main reason to explain the global pattern. Herbaceous crops show that
567 aridity levels have a clear control of the response of the NDVI to drought during the
568 period of vegetation activity. Nevertheless, after the common harvest period (June) this
569 control by aridity mostly disappears. This is also observed in the grasslands and in the
570 sclerophyllous vegetation, and it could be explained by the low vegetation activity of
571 the herbaceous and shrub species during the summer, given the phenological strategies
572 to cope with water stress with the formation of the seeds before the period of dryness
573 (Chaves et al., 2003). The limiting aridity conditions that characterises the regions in
574 which these vegetation types grow would also contribute to explain this phenomenon.
575 On the contrary, the forests, both broad-leaved and coniferous, also show a control by
576 aridity in the relationship between the NDVI and the SPEI during the summer months
577 since these land cover types show the peak of the vegetation activity during this season.

578 In any case, it is also remarkable that the spatial pattern of the NDVI sensitivity to
579 drought in forests is less controlled by aridity during the summer season, curiously the
580 season in which there are more limiting conditions. This could be explained by the
581 NDVI saturation under high levels of leaf area index (Carlson and Ripley, 1997), since



582 once the tree tops are completely foliated the electromagnetic signal is not sensitive to
583 additional leaf growth. This could explain the less sensitive response of the forests to
584 drought in comparison to land cover types characterised by lower leaf area (e.g. shrubs
585 or grasslands). Nevertheless, we do not think that this phenomenon can explain totally
586 the decreased sensitivity to drought with aridity in summer since the dominant
587 coniferous and broad-leaved forests in Spain are usually not characterised by a 100%
588 leaf coverage (Castro-Díez et al., 1997; Molina and del Campo, 2012), so large signal
589 saturation problems are not expected. On the other hand, the ecophysiological strategies
590 of forests to cope with drought may help explain the observed lower relationship
591 between aridity during the summer months. Experimental studies suggested that the
592 interannual variability of the secondary growth could be more sensitive to drought than
593 the sensitivity observed by the photosynthetic activity and the leaf area (Newberry,
594 2010). This could be a strategy to optimize the storage of carbohydrates, suggesting that
595 forests in dry years would prioritize the development of an adequate foliar area in
596 relation to the wood formation in order to maintain respiration and photosynthetic
597 processes. Recent studies by Gazol et al. (2018) and Peña-Gallardo et al. (2018b)
598 confirmed that, irrespective of forest species, there is a higher sensitivity of tree-ring
599 growth to drought, as compared to the sensitivity of the NDVI. The different spatial and
600 seasonal responses of vegetation activity to drought in our study domain can also be
601 linked to the dominant forest species and species richness, which has been evident in
602 numerous studies (e.g. Lloret et al., 2007). Moreover, this might also be attributed to the
603 ecosystem physiological processes, given that vegetation tends to maintain the same
604 water use efficiency under water stress conditions, regardless of vegetation types and
605 environmental conditions (Huxman et al., 2004). This would explain that -
606 independently of the aridity conditions- the response of the NDVI to drought would be



607 similar. Here, we demonstrated that the response of the NDVI to drought is similar
608 during summer months, even with the different land cover types and environmental
609 conditions.

610 A relevant finding of this study is that the response of the NDVI is highly dependent on
611 the time scale at which drought is quantified. Numerous studies indicated that the
612 accumulation of precipitation deficits during different time periods is essential to
613 determine the influence of drought on the NDVI (e.g. Malo and Nicholson, 1990; Liu
614 and Kogan, 1996; Lotsch et al., 2003; Ji and Peters, 2003; Wang et al., 2003). This is
615 simply because soil moisture is impacted largely by precipitation and the atmospheric
616 evaporative demand over previous cumulative periods (Scaini et al., 2015). Moreover,
617 the different morphological, physiological and phenological strategies would also
618 explain the varying response of vegetation types to different drought time scales. This
619 finding is confirmed in previous works using NDVI and different time scales of a
620 drought index (e.g. Ji and Peters, 2003; Vicente-Serrano, 2007), but also using other
621 variables like tree-ring growth (e.g. Pasho et al., 2011; Arzac et al., 2016; Vicente-
622 Serrano et al., 2014a). This study confirms this finding, given that there is a high spatial
623 diversity in the SPEI time scale at which vegetation has its maximum correlation with
624 the NDVI. These spatial variations, combined with strong seasonal differences, are
625 mainly controlled by the dominant land cover types and aridity conditions. In their
626 global assessment, Vicente-Serrano et al. (2013) found gradients in the response of the
627 world biomes to drought, which are driven mainly by the time scale at which the biome
628 responds to drought in a gradient of aridity. Again, the response to these different time
629 scales implies not only different vulnerabilities of vegetation to water deficits, but also
630 various strategies from plants to cope with drought. In Spain, we showed that the NDVI
631 responds mostly to the SPEI at time scales around 20 semi-monthly periods (10



632 months), but with some few seasonal differences (i.e. shorter time scales in spring and
633 early autumn than in late summer and autumn). Herein, it is also noteworthy indicating
634 that there are differences in this response, as a function of land cover types. Overall,
635 during the periods of highest vegetation activity, the herbaceous land covers (e.g. non-
636 irrigated arable lands and grasslands) respond to shorter SPEI time-scales than other
637 forest types. This pattern can be seen in the context that herbaceous covers are more
638 dependent on the weather conditions recorded during short periods. These vegetation
639 types could not reach deep soil levels, which are driven by climatic conditions during
640 longer periods (Changnon and Easterling, 1989; Berg et al., 2017). In contrast, the tree
641 root systems would access to these deeper levels, having the capacity of buffering the
642 effect of short term droughts, albeit with more vulnerability to long droughts that
643 ultimately would affect deep soil moisture levels. This pattern has been recently
644 observed in southeastern Spain when comparing herbaceous crops and vineyards
645 (Contreras and Hunink, 2015). Recently, Okin et al. (2018) linked the different
646 responses to drought time scales between scrubs and chaparral herbaceous vegetation in
647 California to soil water depletion at different levels.

648 Albeit with these general patterns, we also found some relevant seasonal patterns. For
649 example, irrigated lands responded to long SPEI time scales (> 15 months) during
650 summer months, whilst they responded to shorter time scales (<7 months) during spring
651 and autumn. This behaviour can be linked to water management in these areas. In
652 specific, during spring months, these areas do not receive irrigation and accordingly
653 vegetation activity is determined by water stored in the soil. On the contrary, summer
654 irrigation depends on the water stored in the dense net of reservoirs existing in Spain;
655 some of them have a multiannual capacity. Water availability in the reservoirs usually
656 depends on the climate conditions recorded during long periods (one or two years)



657 (López-Moreno et al., 2004; Lorenzo-Lacruz et al., 2010), which determine water
658 availability for irrigation. This explains why vegetation activity in irrigated lands
659 depends on long time scales of drought. Similarly, vineyards and olive groves respond
660 to long SPEI time-scales during summer. These cultivations are highly resistant to
661 drought stress (Quiroga and Iglesias, 2009). However, these adapted cultivations can be
662 sensitive to severe droughts under extreme summer dryness. In comparison to other
663 natural vegetation, mixed forests show response to shorter SPEI time scales. This could
664 be explained by the low resistance of these forest species to water deficits [e.g. the
665 different fir species located in humid mountain areas, (Camarero et al., 2011; Camarero
666 et al., 2018)].

667 Here, we also showed that climate aridity can partially explain the response of the
668 NDVI to the different SPEI time scales. In Spain, the range of the mean aridity recorded
669 by the mean land cover types is much lower than that observed at the global scale for
670 the world biomes (Vicente-Serrano et al., 2013). This might explain why there are no
671 clear patterns in the response of the land cover types to the aridity gradients and the
672 SPEI time scales at which the maximum correlation between the NDVI and SPEI is
673 found. Nevertheless, we found some seasonal differences between the cold and warm
674 seasons. In summer, the NDVI responds to longer SPEI time scales, as opposed to the
675 most humid forests that respond to shorter time scales. This stresses that – in addition to
676 aridity- the degree of vulnerability to different duration water deficits, which are well-
677 quantified using the drought time scales, may contribute to explaining the spatial
678 distribution of the main land cover types across Spain given different biophysical
679 conditions, but also the different strategies of vegetation types to cope with water stress
680 (Chaves et al., 2003; McDowell et al., 2008), which are strongly variable in complex
681 Mediterranean ecosystems.



682 Acknowledgements

683 This work was supported by the research projects PCIN-2015-220, CGL2014-52135-
684 C03-01 and CGL2017-82216-R financed by the Spanish Commission of Science and
685 Technology and FEDER. IMDROFLOOD financed by the Water Works 2014 co-
686 funded all of the European Commission and INDECIS, which is part of ERA4CS, an
687 ERA-NET initiated by JPI Climate, and funded by FORMAS (Sweden), DLR
688 (Germany), BMFWF(Austria), IFD (Denmark), MINECO(Spain) and ANR (France),
689 with co-funding by the European Union (Grant 690462), FORWARD financed under
690 the ERA-NET Cofund WaterWorks2015 Call EU and Innovation Fund Denmark (IFD).
691 This ERA-NET is an integral part of the 2016 Joint Activities developed by the Water
692 Challenges for a Changing World Joint Programme Initiative (Water JPI). Marina Peña-
693 Gallardo was supported by the Spanish Ministry of Economy and Competitiveness
694

695 References

- 696 Abrams, M. D., Schultz, J. C. and Kleiner, K. W.: Ecophysiological responses in mesic
697 versus xeric hardwood species to an early-season drought in central Pennsylvania, *For.*
698 *Sci.*, 36(4), 970–981, 1990.
- 699 Allen, C. D., Macalady, A. K., Chenchouni, H., Bachelet, D., McDowell, N., Venetier,
700 M., Kitzberger, T., Rigling, A., Breshears, D. D., Hogg, E. H. (T. ., Gonzalez, P.,
701 Fensham, R., Zhang, Z., Castro, J., Demidova, N., Lim, J.-H., Allard, G., Running, S.
702 W., Semerci, A. and Cobb, N.: A global overview of drought and heat-induced tree
703 mortality reveals emerging climate change risks for forests, *For. Ecol. Manage.*, 259(4),
704 660–684, doi:10.1016/j.foreco.2009.09.001, 2010.
- 705 Allen, C. D., Breshears, D. D. and McDowell, N. G.: On underestimation of global
706 vulnerability to tree mortality and forest die-off from hotter drought in the
707 Anthropocene, *Ecosphere*, 6(8), doi:10.1890/ES15-00203.1, 2015.
- 708 Allen, R. G., Pereira, L. S., Raes, D. and Smith, M.: No Title, *Crop Evapotranspiration*
709 *Guidel. Comput. Crop Water Requir.*, 1998.
- 710 Anyamba, A. and Tucker, C. J.: Analysis of Sahelian vegetation dynamics using
711 NOAA-AVHRR NDVI data from 1981-2003, *J. Arid Environ.*, 63(3), 596–614,
712 doi:10.1016/j.jaridenv.2005.03.007, 2005.
- 713 Arzac, A., García-Cervigón, A. I., Vicente-Serrano, S. M., Loidi, J. and Olano, J. M.:
714 Phenological shifts in climatic response of secondary growth allow *Juniperus sabina* L.
715 to cope with altitudinal and temporal climate variability, *Agric. For. Meteorol.*, 217,
716 doi:10.1016/j.agrformet.2015.11.011, 2016.
- 717 Asseng, S., Ewert, F., Martre, P., Rötter, R. P., Lobell, D. B., Cammarano, D., Kimball,
718 B. A., Ottman, M. J., Wall, G. W., White, J. W., Reynolds, M. P., Alderman, P. D.,
719 Prasad, P. V. V., Aggarwal, P. K., Anothai, J., Basso, B., Biernath, C., Challinor, A. J.,
720 De Sanctis, G., Doltra, J., Fereres, E., Garcia-Vila, M., Gayler, S., Hoogenboom, G.,
721 Hunt, L. A., Izaurrealde, R. C., Jabloun, M., Jones, C. D., Kersebaum, K. C., Koehler,
722 A.-K., Müller, C., Naresh Kumar, S., Nendel, C., O’leary, G., Olesen, J. E., Palosuo, T.,
723 Priesack, E., Eyshi Rezaei, E., Ruane, A. C., Semenov, M. A., Shcherbak, I., Stöckle,
724 C., Stratonovitch, P., Streck, T., Supit, I., Tao, F., Thorburn, P. J., Waha, K., Wang, E.,
725 Wallach, D., Wolf, J., Zhao, Z. and Zhu, Y.: Rising temperatures reduce global wheat
726 production, *Nat. Clim. Chang.*, 5(2), 143–147, doi:10.1038/nclimate2470, 2015.



- 727 Austin, R. B., Cantero-Martínez, C., Arrúe, J. L., Playán, E. and Cano-Marcellán, P.:
728 Yield-rainfall relationships in cereal cropping systems in the Ebro river valley of Spain,
729 *Eur. J. Agron.*, 8(3–4), 239–248, doi:10.1016/S1161-0301(97)00063-4, 1998.
- 730 Bachmair, S., Kohn, I. and Stahl, K.: Exploring the link between drought indicators and
731 impacts, *Nat. Hazards Earth Syst. Sci.*, 15(6), 1381–1397, doi:10.5194/nhess-15-1381-
732 2015, 2015.
- 733 Bachmair, S., Tanguy, M., Hannaford, J. and Stahl, K.: How well do meteorological
734 indicators represent agricultural and forest drought across Europe?, *Environ. Res. Lett.*,
735 13(3), doi:10.1088/1748-9326/aaafda, 2018.
- 736 Bailing, M., Zhiyong, L., Cunzhu, L., Lixin, W., Chengzhen, J., Fuxiang, B. and Chao,
737 J.: Temporal and spatial heterogeneity of drought impact on vegetation growth on the
738 Inner Mongolian Plateau, *Rangel. J.*, 40(2), 113–128, doi:10.1071/RJ16097, 2018.
- 739 Baldocchi, D. D., Xu, L. and Kiang, N.: How plant functional-type, weather, seasonal
740 drought, and soil physical properties alter water and energy fluxes of an oak-grass
741 savanna and an annual grassland, *Agric. For. Meteorol.*, 123(1–2), 13–39,
742 doi:10.1016/j.agrformet.2003.11.006, 2004.
- 743 Barbosa, H. A., Huete, A. R. and Baethgen, W. E.: A 20-year study of NDVI variability
744 over the Northeast Region of Brazil, *J. Arid Environ.*, 67(2), 288–307,
745 doi:10.1016/j.jaridenv.2006.02.022, 2006.
- 746 Barker, L. J., Hannaford, J., Chiverton, A. and Svensson, C.: From meteorological to
747 hydrological drought using standardised indicators, *Hydrol. Earth Syst. Sci.*, 20(6),
748 2483–2505, doi:10.5194/hess-20-2483-2016, 2016.
- 749 del Barrio, G., Puigdefabregas, J., Sanjuan, M. E., Stellmes, M. and Ruiz, A.:
750 Assessment and monitoring of land condition in the Iberian Peninsula, 1989–2000,
751 *Remote Sens. Environ.*, 114(8), 1817–1832, doi:10.1016/j.rse.2010.03.009, 2010.
- 752 Berg, A., Sheffield, J. and Milly, P. C. D.: Divergent surface and total soil moisture
753 projections under global warming, *Geophys. Res. Lett.*, 44(1), 236–244,
754 doi:10.1002/2016GL071921, 2017.
- 755 Bhuiyan, C., Singh, R. P. and Kogan, F. N.: Monitoring drought dynamics in the
756 Aravalli region (India) using different indices based on ground and remote sensing data,
757 *Int. J. Appl. Earth Obs. Geoinf.*, 8(4), 289–302, doi:10.1016/j.jag.2006.03.002, 2006.
- 758 Breshears, D. D., Cobb, N. S., Rich, P. M., Price, K. P., Allen, C. D., Balice, R. G.,
759 Romme, W. H., Kastens, J. H., Floyd, M. L., Belnap, J., Anderson, J. J., Myers, O. B.
760 and Meyer, C. W.: Regional vegetation die-off in response to global-change-type
761 drought, *Proc. Natl. Acad. Sci. U. S. A.*, 102(42), 15144–15148,
762 doi:10.1073/pnas.0505734102, 2005.
- 763 Camarero, J. J., Bigler, C., Linares, J. C. and Gil-Pelegrín, E.: Synergistic effects of past
764 historical logging and drought on the decline of Pyrenean silver fir forests, *For. Ecol.
765 Manage.*, 262(5), 759–769, doi:10.1016/j.foreco.2011.05.009, 2011.
- 766 Camarero, J. J., Gazol, A., Sangüesa-Barreda, G., Oliva, J. and Vicente-Serrano, S. M.:
767 To die or not to die: Early warnings of tree dieback in response to a severe drought, *J.
768 Ecol.*, 103(1), doi:10.1111/1365-2745.12295, 2015.
- 769 Camarero, J. J., Gazol, A., Sangüesa-Barreda, G., Cantero, A., Sánchez-Salguero, R.,
770 Sánchez-Miranda, A., Granda, E., Serra-Maluquer, X. and Ibáñez, R.: Forest growth
771 responses to drought at short- and long-term scales in Spain: Squeezing the stress



- 772 memory from tree rings, *Front. Ecol. Evol.*, 6(FEB), doi:10.3389/fevo.2018.00009,
773 2018.
- 774 Carlson, T. N. and Ripley, D. A.: On the relation between NDVI, fractional vegetation
775 cover, and leaf area index, *Remote Sens. Environ.*, 62(3), 241–252, doi:10.1016/S0034-
776 4257(97)00104-1, 1997.
- 777 Carnicer, J., Coll, M., Ninyerola, M., Pons, X., Sánchez, G. and Peñuelas, J.:
778 Widespread crown condition decline, food web disruption, and amplified tree mortality
779 with increased climate change-type drought, *Proc. Natl. Acad. Sci. U. S. A.*, 108(4),
780 1474–1478, doi:10.1073/pnas.1010070108, 2011.
- 781 Castro-Díez, P., Villar-Salvador, P., Pérez-Rantomé, C., Maestro-Martínez, M. and
782 Montserrat-Martí, G.: Leaf morphology and leaf chemical composition in three *Quercus*
783 (*Fagaceae*) species along a rainfall gradient in NE Spain, *Trees - Struct. Funct.*, 11(3),
784 127–134, doi:10.1007/s004680050068, 1997.
- 785 Changnon, S. A. and Easterling, W. E.: MEASURING DROUGHT IMPACTS: THE
786 ILLINOIS CASE, *JAWRA J. Am. Water Resour. Assoc.*, 25(1), 27–42,
787 doi:10.1111/j.1752-1688.1989.tb05663.x, 1989.
- 788 Chaves, M. M., Maroco, J. P. and Pereira, J. S.: Understanding plant responses to
789 drought - From genes to the whole plant, *Funct. Plant Biol.*, 30(3), 239–264,
790 doi:10.1071/FP02076, 2003.
- 791 Ciais, P., Reichstein, M., Viovy, N., Granier, A., Ogée, J., Allard, V., Aubinet, M.,
792 Buchmann, N., Bernhofer, C., Carrara, A., Chevallier, F., De Noblet, N., Friend, A. D.,
793 Friedlingstein, P., Grünwald, T., Heinesch, B., Keronen, P., Knohl, A., Krinner, G.,
794 Loustau, D., Manca, G., Matteucci, G., Miglietta, F., Ourcival, J. M., Papale, D.,
795 Pilegaard, K., Rambal, S., Seufert, G., Soussana, J. F., Sanz, M. J., Schulze, E. D.,
796 Vesala, T. and Valentini, R.: Europe-wide reduction in primary productivity caused by
797 the heat and drought in 2003, *Nature*, 437(7058), 529–533, doi:10.1038/nature03972,
798 2005.
- 799 Contreras, S. and Hunink, J. E.: Drought effects on rainfed agriculture using
800 standardized indices: A case study in SE Spain, in *Drought: Research and Science-
801 Policy Interfacing - Proceedings of the International Conference on Drought: Research
802 and Science-Policy Interfacing*, pp. 65–70., 2015.
- 803 Dardel, C., Kergoat, L., Hiernaux, P., Mougín, E., Grippa, M. and Tucker, C. J.: Re-
804 greening Sahel: 30 years of remote sensing data and field observations (Mali, Niger),
805 *Remote Sens. Environ.*, 140, 350–364, doi:10.1016/j.rse.2013.09.011, 2014.
- 806 Fischer, E. M., Seneviratne, S. I., Vidale, P. L., Lüthi, D. and Schär, C.: Soil moisture-
807 atmosphere interactions during the 2003 European summer heat wave, *J. Clim.*, 20(20),
808 5081–5099, doi:10.1175/JCLI4288.1, 2007.
- 809 García-Haro, F. J., Campos-Taberner, M., Sabater, N., Belda, F., Moreno, A., Gilabert,
810 M. A., Martínez, B., Pérez-Hoyos, A. and Meliá, J.: Vegetation vulnerability to drought
811 in Spain | Vulnerabilidad de la vegetación a la sequía en España, *Rev. Teledetec.*, (42),
812 29–37, doi:10.4995/raet.2014.2283, 2014.
- 813 García, M., Litago, J., Palacios-Orueta, A., Pinzón, J. E. and Ustin Susan, L.: Short-term
814 propagation of rainfall perturbations on terrestrial ecosystems in central California,
815 *Appl. Veg. Sci.*, 13(2), 146–162, doi:10.1111/j.1654-109X.2009.01057.x, 2010.
- 816 Gazol, A., Camarero, J. J., Anderegg, W. R. L. and Vicente-Serrano, S. M.: Impacts of



- 817 droughts on the growth resilience of Northern Hemisphere forests, *Glob. Ecol.*
818 *Biogeogr.*, 26(2), doi:10.1111/geb.12526, 2017.
- 819 Gazol, A., Camarero, J. J., Vicente-Serrano, S. M., Sánchez-Salguero, R., Gutiérrez, E.,
820 de Luis, M., Sangüesa-Barreda, G., Novak, K., Rozas, V., Tíscar, P. A., Linares, J. C.,
821 Martín-Hernández, N., Martínez del Castillo, E., Ribas, M., García-González, I., Silla,
822 F., Camisón, A., Génova, M., Olano, J. M., Longares, L. A., Hevia, A., Tomás-
823 Burguera, M. and Galván, J. D.: Forest resilience to drought varies across biomes, *Glob.*
824 *Chang. Biol.*, 24(5), doi:10.1111/gcb.14082, 2018.
- 825 Gessner, U., Naeimi, V., Klein, I., Kuenzer, C., Klein, D. and Dech, S.: The relationship
826 between precipitation anomalies and satellite-derived vegetation activity in Central
827 Asia, *Glob. Planet. Change*, 110, 74–87, doi:10.1016/j.gloplacha.2012.09.007, 2013.
- 828 González-Alonso, F. and Casanova, J. L.: Application of NOAA-AVHRR images for
829 the validation and risk assessment of natural disasters in Spain, in *Remote Sensing '96*,
830 pp. 227–233, Balkema, Rotterdam., 1997.
- 831 González-Hidalgo, J. C., Vicente-Serrano, S. M., Peña-Angulo, D., Salinas, C., Tomas-
832 Burguera, M. and Beguería, S.: High-resolution spatio-temporal analyses of drought
833 episodes in the western Mediterranean basin (Spanish mainland, Iberian Peninsula),
834 *Acta Geophys.*, 66(3), doi:10.1007/s11600-018-0138-x, 2018.
- 835 Gouveia, C. M., Bastos, A., Trigo, R. M. and Dacamara, C. C.: Drought impacts on
836 vegetation in the pre- and post-fire events over Iberian Peninsula, *Nat. Hazards Earth*
837 *Syst. Sci.*, 12(10), 3123–3137, doi:10.5194/nhess-12-3123-2012, 2012.
- 838 Gouveia, C. M., Páscoa, P., Russo, A. and Trigo, R. M.: Land degradation trend
839 assessment over iberia during 1982-2012 | Evaluación de la tendencia a la degradación
840 del suelo en Iberia durante 1982-2012, *Cuad. Investig. Geogr.*, 42(1), 89–112,
841 doi:10.18172/cig.2808, 2016.
- 842 Gouveia, C. M., Trigo, R. M., Beguería, S. and Vicente-Serrano, S. M.: Drought
843 impacts on vegetation activity in the Mediterranean region: An assessment using remote
844 sensing data and multi-scale drought indicators, *Glob. Planet. Change*, 151,
845 doi:10.1016/j.gloplacha.2016.06.011, 2017.
- 846 Grissino-Mayer, H. D. and Fritts, H. C.: The International Tree-Ring Data Bank: An
847 enhanced global database serving the global scientific community, *Holocene*, 7(2), 235–
848 238, doi:10.1177/095968369700700212, 1997.
- 849 Gu, Y., Brown, J. F., Verdin, J. P. and Wardlow, B.: A five-year analysis of MODIS
850 NDVI and NDWI for grassland drought assessment over the central Great Plains of the
851 United States, *Geophys. Res. Lett.*, 34(6), doi:10.1029/2006GL029127, 2007.
- 852 Herrmann, S. M., Anyamba, A. and Tucker, C. J.: Recent trends in vegetation dynamics
853 in the African Sahel and their relationship to climate, *Glob. Environ. Chang.*, 15(4),
854 394–404, doi:10.1016/j.gloenvcha.2005.08.004, 2005.
- 855 Herrmann, S. M., Didan, K., Barreto-Munoz, A. and Crimmins, M. A.: Divergent
856 responses of vegetation cover in Southwestern US ecosystems to dry and wet years at
857 different elevations, *Environ. Res. Lett.*, 11(12), doi:10.1088/1748-9326/11/12/124005,
858 2016.
- 859 Hill, J., Stellmes, M., Udelhoven, T., Röder, A. and Sommer, S.: Mediterranean
860 desertification and land degradation. Mapping related land use change syndromes based
861 on satellite observations, *Glob. Planet. Change*, 64(3–4), 146–157,



- 862 doi:10.1016/j.gloplacha.2008.10.005, 2008.
- 863 Hirschi, M., Seneviratne, S. I., Alexandrov, V., Boberg, F., Boroneant, C., Christensen,
864 O. B., Formayer, H., Orłowsky, B. and Stepanek, P.: Observational evidence for soil-
865 moisture impact on hot extremes in southeastern Europe, *Nat. Geosci.*, 4(1), 17–21,
866 doi:10.1038/ngeo1032, 2011.
- 867 Huete, A., Didan, K., Miura, T., Rodriguez, E. P., Gao, X. and Ferreira, L. G.:
868 Overview of the radiometric and biophysical performance of the MODIS vegetation
869 indices, *Remote Sens. Environ.*, 83(1–2), 195–213, doi:10.1016/S0034-4257(02)00096-
870 2, 2002.
- 871 Huxman, T. E., Smith, M. D., Fay, P. A., Knapp, A. K., Shaw, M. R., Lolk, M. E.,
872 Smith, S. D., Tissue, D. T., Zak, J. C., Weltzin, J. F., Pockman, W. T., Sala, O. E.,
873 Haddad, B. M., Harte, J., Koch, G. W., Schwinning, S., Small, E. E. and Williams, D.
874 G.: Convergence across biomes to a common rain-use efficiency, *Nature*, 429(6992),
875 651–654, doi:10.1038/nature02561, 2004.
- 876 Iglesias, E., Garrido, A. and Gómez-Ramos, A.: Evaluation of drought management in
877 irrigated areas, *Agric. Econ.*, 29(2), 211–229, doi:10.1016/S0169-5150(03)00084-7,
878 2003.
- 879 Ivits, E., Horion, S., Fensholt, R. and Cherlet, M.: Drought footprint on European
880 ecosystems between 1999 and 2010 assessed by remotely sensed vegetation phenology
881 and productivity, *Glob. Chang. Biol.*, 20(2), 581–593, doi:10.1111/gcb.12393, 2014.
- 882 Jenkins, J. C., Chojnacky, D. C., Heath, L. S. and Birdsey, R. A.: National-scale
883 biomass estimators for United States tree species, *For. Sci.*, 49(1), 12–35, 2003.
- 884 Ji, L. and Peters, A. J.: Assessing vegetation response to drought in the northern Great
885 Plains using vegetation and drought indices, *Remote Sens. Environ.*, 87(1), 85–98,
886 doi:10.1016/S0034-4257(03)00174-3, 2003.
- 887 Julien, Y., Sobrino, J. A., Mattar, C., Ruescas, A. B., Jiménez-Muñoz, J. C., Sòria, G.,
888 Hidalgo, V., Atitar, M., Franch, B. and Cuenca, J.: Temporal analysis of normalized
889 difference vegetation index (NDVI) and land surface temperature (LST) parameters to
890 detect changes in the Iberian land cover between 1981 and 2001, *Int. J. Remote Sens.*,
891 32(7), 2057–2068, doi:10.1080/01431161003762363, 2011.
- 892 De Keersmaecker, W., Lhermitte, S., Hill, M. J., Tits, L., Coppin, P. and Somers, B.:
893 Assessment of regional vegetation response to climate anomalies: A case study for
894 australia using GIMMS NDVI time series between 1982 and 2006, *Remote Sens.*, 9(1),
895 doi:10.3390/rs9010034, 2017.
- 896 Knipling, E. B.: Physical and physiological basis for the reflectance of visible and near-
897 infrared radiation from vegetation, *Remote Sens. Environ.*, 1(3), 155–159,
898 doi:10.1016/S0034-4257(70)80021-9, 1970.
- 899 Kogan, F. N.: Global Drought Watch from Space, *Bull. Am. Meteorol. Soc.*, 78(4),
900 621–636, doi:10.1175/1520-0477(1997)078<0621:GDWFS>2.0.CO;2, 1997.
- 901 Lasanta, T. and Vicente-Serrano, S. M.: Complex land cover change processes in
902 semiarid Mediterranean regions: An approach using Landsat images in northeast Spain,
903 *Remote Sens. Environ.*, 124, doi:10.1016/j.rse.2012.04.023, 2012.
- 904 Lasanta, T., Arnáez, J., Pascual, N., Ruiz-Flaño, P., Errea, M. P. and Lana-Renault, N.:
905 Space–time process and drivers of land abandonment in Europe, *Catena*, 149, 810–823,
906 doi:10.1016/j.catena.2016.02.024, 2017.



- 907 Liu, N., Harper, R. J., Dell, B., Liu, S. and Yu, Z.: Vegetation dynamics and rainfall
908 sensitivity for different vegetation types of the Australian continent in the dry period
909 2002–2010, *Ecohydrology*, 10(2), doi:10.1002/eco.1811, 2017.
- 910 Liu, W. T. and Kogan, F. N.: Monitoring regional drought using the vegetation
911 condition index, *Int. J. Remote Sens.*, 17(14), 2761–2782,
912 doi:10.1080/01431169608949106, 1996.
- 913 Lloret, F., Lobo, A., Estevan, H., Maisongrande, P., Vayreda, J. and Terradas, J.:
914 Woody plant richness and NDVI response to drought events in Catalonian (northeastern
915 Spain) forests, *Ecology*, 88(9), 2270–2279, doi:10.1890/06-1195.1, 2007.
- 916 Lobell, D. B., Hammer, G. L., Chenu, K., Zheng, B., Mclean, G. and Chapman, S. C.:
917 The shifting influence of drought and heat stress for crops in northeast Australia, *Glob.*
918 *Chang. Biol.*, 21(11), 4115–4127, doi:10.1111/gcb.13022, 2015.
- 919 López-Moreno, J. I., Beguería, S. and García-Ruiz, J. M.: The management of a large
920 Mediterranean reservoir: Storage regimes of the Yesa Reservoir, Upper Aragon River
921 basin, Central Spanish Pyrenees, *Environ. Manage.*, 34(4), 508–515,
922 doi:10.1007/s00267-003-0249-1, 2004.
- 923 López-Moreno, J. I., Vicente-Serrano, S. M., Zabalza, J., Beguería, S., Lorenzo-Lacruz,
924 J., Azorin-Molina, C. and Morán-Tejeda, E.: Hydrological response to climate
925 variability at different time scales: A study in the Ebro basin, *J. Hydrol.*, 477, 175–188,
926 doi:10.1016/j.jhydrol.2012.11.028, 2013.
- 927 Lorenzo-Lacruz, J., Vicente-Serrano, S. M., López-Moreno, J. I., Beguería, S., García-
928 Ruiz, J. M. and Cuadrat, J. M.: The impact of droughts and water management on
929 various hydrological systems in the headwaters of the Tagus River (central Spain), *J.*
930 *Hydrol.*, 386(1–4), doi:10.1016/j.jhydrol.2010.01.001, 2010.
- 931 Lorenzo-Lacruz, J., Morán-Tejeda, E., Vicente-Serrano, S. M. and López-Moreno, J. I.:
932 Streamflow droughts in the Iberian Peninsula between 1945 and 2005: Spatial and
933 temporal patterns, *Hydrol. Earth Syst. Sci.*, 17(1), doi:10.5194/hess-17-119-2013, 2013.
- 934 Lotsch, A., Friedl, M. A., Anderson, B. T. and Tucker, C. J.: Coupled vegetation-
935 precipitation variability observed from satellite and climate records, *Geophys. Res.*
936 *Let.*, 30(14), doi:10.1029/2003GL017506, 2003.
- 937 Ma, X., Huete, A., Moran, S., Ponce-Campos, G. and Eamus, D.: Abrupt shifts in
938 phenology and vegetation productivity under climate extremes, *J. Geophys. Res.*
939 *Biogeosciences*, 120(10), 2036–2052, doi:10.1002/2015JG003144, 2015.
- 940 Malo, A. R. and Nicholson, S. E.: A study of rainfall and vegetation dynamics in the
941 African Sahel using normalized difference vegetation index, *J. Arid Environ.*, 19(1), 1–
942 24, 1990.
- 943 Martínez-Fernández, J. and Ceballos, A.: Temporal Stability of Soil Moisture in a
944 Large-Field Experiment in Spain, *Soil Sci. Soc. Am. J.*, 67(6), 1647–1656, 2003.
- 945 McDowell, N., Pockman, W. T., Allen, C. D., Breshears, D. D., Cobb, N., Kolb, T.,
946 Plaut, J., Sperry, J., West, A., Williams, D. G. and Yezzer, E. A.: Mechanisms of plant
947 survival and mortality during drought: Why do some plants survive while others
948 succumb to drought?, *New Phytol.*, 178(4), 719–739, doi:10.1111/j.1469-
949 8137.2008.02436.x, 2008.
- 950 McKee, T. B., Doesken, N. J. and Kleist, J.: The relationship of drought frequency and
951 duration to time scales, *Eighth Conf. Appl. Climatol.*, 179–184, 1993.



- 952 Milich, L. and Weiss, E.: Characterization of the sahel: Implications of correctly
953 calculating interannual coefficients of variation (CoVs) from GAC NDVI values, *Int. J.*
954 *Remote Sens.*, 18(18), 3749–3759, doi:10.1080/014311697216603, 1997.
- 955 Molina, A. J. and del Campo, A. D.: The effects of experimental thinning on throughfall
956 and stemflow: A contribution towards hydrology-oriented silviculture in Aleppo pine
957 plantations, *For. Ecol. Manage.*, 269, 206–213, doi:10.1016/j.foreco.2011.12.037, 2012.
- 958 Mu, Q., Zhao, M., Kimball, J. S., McDowell, N. G. and Running, S. W.: A remotely
959 sensed global terrestrial drought severity index, *Bull. Am. Meteorol. Soc.*, 94(1), 83–98,
960 doi:10.1175/BAMS-D-11-00213.1, 2013.
- 961 Mühlbauer, S., Costa, A. C. and Caetano, M.: A spatiotemporal analysis of droughts and
962 the influence of North Atlantic Oscillation in the Iberian Peninsula based on MODIS
963 imagery, *Theor. Appl. Climatol.*, 124(3–4), 703–721, doi:10.1007/s00704-015-1451-9,
964 2016.
- 965 Mukherjee, S., Mishra, A. and Trenberth, K. E.: Climate Change and Drought: a
966 Perspective on Drought Indices, *Curr. Clim. Change. Reports*, 4(2), 145–163,
967 doi:10.1007/s40641-018-0098-x, 2018.
- 968 Myneni, R. B., Hall, F. G., Sellers, P. J. and Marshak, A. L.: Interpretation of spectral
969 vegetation indexes, *IEEE Trans. Geosci. Remote Sens.*, 33(2), 481–486,
970 doi:10.1109/36.377948, 1995.
- 971 Newberry, T. L.: Effect of climatic variability on $\delta^{13}\text{C}$ and tree-ring growth in piñon
972 pine (*Pinus edulis*), *Trees - Struct. Funct.*, 24(3), 551–559, doi:10.1007/s00468-010-
973 0426-9, 2010.
- 974 Nicholson, S. E., Davenport, M. L. and Malo, A. R.: A comparison of the vegetation
975 response to rainfall in the Sahel and East Africa, using normalized difference vegetation
976 index from NOAA AVHRR, *Clim. Change*, 17(2–3), 209–241,
977 doi:10.1007/BF00138369, 1990.
- 978 Okin, G. S., Dong, C., Willis, K. S., Gillespie, T. W. and MacDonald, G. M.: The
979 Impact of Drought on Native Southern California Vegetation: Remote Sensing Analysis
980 Using MODIS-Derived Time Series, *J. Geophys. Res. Biogeosciences*, 123(6), 1927–
981 1939, doi:10.1029/2018JG004485, 2018.
- 982 Olsen, J. L., Ceccato, P., Proud, S. R., Fensholt, R., Grippa, M., Mougín, B., Ardö, J.
983 and Sandholt, I.: Relation between seasonally detrended shortwave infrared reflectance
984 data and land surface moisture in semi-arid Sahel, *Remote Sens.*, 5(6), 2898–2927,
985 doi:10.3390/rs5062898, 2013.
- 986 Páscoa, P., Gouveia, C. M., Russo, A. and Trigo, R. M.: The role of drought on wheat
987 yield interannual variability in the Iberian Peninsula from 1929 to 2012, *Int. J.*
988 *Biometeorol.*, 61(3), 439–451, doi:10.1007/s00484-016-1224-x, 2017.
- 989 Pasho, E., Camarero, J. J., de Luis, M. and Vicente-Serrano, S. M.: Impacts of drought
990 at different time scales on forest growth across a wide climatic gradient in north-eastern
991 Spain, *Agric. For. Meteorol.*, 151(12), doi:10.1016/j.agrformet.2011.07.018, 2011.
- 992 Pausas, J. G.: Changes in fire and climate in the eastern Iberian Peninsula
993 (Mediterranean Basin), *Clim. Change*, 63(3), 337–350,
994 doi:10.1023/B:CLIM.0000018508.94901.9c, 2004.
- 995 Pausas, J. G. and Fernández-Muñoz, S.: Fire regime changes in the Western
996 Mediterranean Basin: From fuel-limited to drought-driven fire regime, *Clim. Change*,



- 997 110(1–2), 215–226, doi:10.1007/s10584-011-0060-6, 2012.
- 998 Peco, B., Ortega, M. and Levassor, C.: Similarity between seed bank and vegetation in
999 Mediterranean grassland: A predictive model, *J. Veg. Sci.*, 9(6), 815–828,
1000 doi:10.2307/3237047, 1998.
- 1001 Peña-Gallardo, M., Vicente-Serrano, S. M., Camarero, J. J., Gazol, A., Sánchez-
1002 Salguero, R., Domínguez-Castro, F., El Kenawy, A., Beguería-Portugés, S., Gutiérrez,
1003 E., de Luis, M., Sangüesa-Barreda, G., Novak, K., Rozas, V., Tíscar, P. A., Linares, J.
1004 C., del Castillo, E., Ribas Matamoros, M., García-González, I., Silla, F., Camisón, Á.,
1005 Génova, M., Olano, J. M., Longares, L. A., Hevia, A. and Galván, J. D.: Drought
1006 Sensitiveness on Forest Growth in Peninsular Spain and the Balearic Islands, *Forests*,
1007 9(9), 2018a.
- 1008 Peña-Gallardo, M., SM, V.-S., Domínguez-Castro, F., Quiring, S., Svoboda, M.,
1009 Beguería, S. and Hannaford, J.: Effectiveness of drought indices in identifying impacts
1010 on major crops across the USA, *Clim. Res.*, 75(3), 221–240 [online] Available from:
1011 <https://www.int-res.com/abstracts/cr/v75/n3/p221-240/>, 2018b.
- 1012 Pinzon, J. E. and Tucker, C. J.: A non-stationary 1981-2012 AVHRR
1013 NDVI<inf>3g</inf>-time series, *Remote Sens.*, 6(8), 6929–6960,
1014 doi:10.3390/rs6086929, 2014.
- 1015 Quiring, S. M. and Ganesh, S.: Evaluating the utility of the Vegetation Condition Index
1016 (VCI) for monitoring meteorological drought in Texas, *Agric. For. Meteorol.*, 150(3),
1017 330–339, doi:10.1016/j.agrformet.2009.11.015, 2010.
- 1018 Quiroga, S. and Iglesias, A.: A comparison of the climate risks of cereal, citrus,
1019 grapevine and olive production in Spain, *Agric. Syst.*, 101(1–2), 91–100,
1020 doi:10.1016/j.agsy.2009.03.006, 2009.
- 1021 Reichstein, M., Ciais, P., Papale, D., Valentini, R., Running, S., Viovy, N., Cramer, W.,
1022 Granier, A., Ogée, J., Allard, V., Aubinet, M., Bernhofer, C., Buchmann, N., Carrara,
1023 A., Grünwald, T., Heimann, M., Heinesch, B., Knohl, A., Kutsch, W., Loustau, D.,
1024 Manca, G., Matteucci, G., Miglietta, F., Ourcival, J. M., Pilegaard, K., Pumpanen, J.,
1025 Rambal, S., Schaphoff, S., Seufert, G., Soussana, J.-F., Sanz, M.-J., Vesala, T. and
1026 Zhao, M.: Reduction of ecosystem productivity and respiration during the European
1027 summer 2003 climate anomaly: A joint flux tower, remote sensing and modelling
1028 analysis, *Glob. Chang. Biol.*, 13(3), 634–651, doi:10.1111/j.1365-2486.2006.01224.x,
1029 2007.
- 1030 Restaino, C. M., Peterson, D. L. and Littell, J.: Increased water deficit decreases
1031 Douglas fir growth throughout western US forests, *Proc. Natl. Acad. Sci. U. S. A.*,
1032 113(34), 9557–9562, doi:10.1073/pnas.1602384113, 2016.
- 1033 Rhee, J., Im, J. and Carbone, G. J.: Monitoring agricultural drought for arid and humid
1034 regions using multi-sensor remote sensing data, *Remote Sens. Environ.*, 114(12), 2875–
1035 2887, doi:10.1016/j.rse.2010.07.005, 2010.
- 1036 Russi, L., Cocks, P. S. and Roberts, E. H.: Seed bank dynamics in a Mediterranean
1037 grassland, *J. Appl. Ecol.*, 29(3), 763–771, doi:10.2307/2404486, 1992.
- 1038 Scaini, A., Sánchez, N., Vicente-Serrano, S. M. and Martínez-Fernández, J.: SMOS-
1039 derived soil moisture anomalies and drought indices: A comparative analysis using in
1040 situ measurements, *Hydrol. Process.*, 29(3), doi:10.1002/hyp.10150, 2015.
- 1041 Schultz, P. A. and Halpert, M. S.: Global analysis of the relationships among a



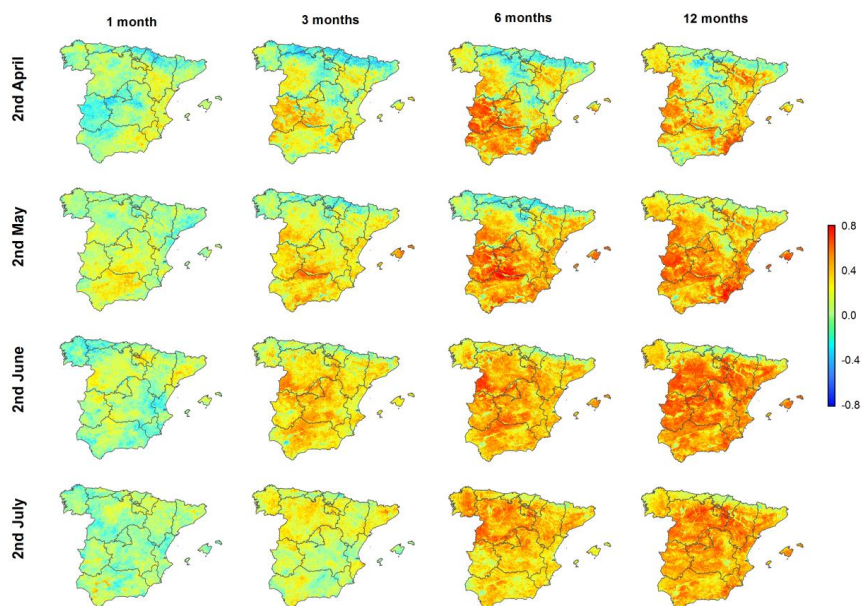
- 1042 vegetation index, precipitation and land surface temperature, *Int. J. Remote Sens.*,
1043 16(15), 2755–2777, doi:10.1080/01431169508954590, 1995.
- 1044 Slayback, D. A., Pinzon, J. E., Los, S. O. and Tucker, C. J.: Northern hemisphere
1045 photosynthetic trends 1982-99, *Glob. Chang. Biol.*, 9(1), 1–15, doi:10.1046/j.1365-
1046 2486.2003.00507.x, 2003.
- 1047 Sona, N. T., Chen, C. F., Chen, C. R., Chang, L. Y. and Minh, V. Q.: Monitoring
1048 agricultural drought in the lower mekong basin using MODIS NDVI and land surface
1049 temperature data, *Int. J. Appl. Earth Obs. Geoinf.*, 18(1), 417–427,
1050 doi:10.1016/j.jag.2012.03.014, 2012.
- 1051 Stagge, J. H., Kohn, I., Tallaksen, L. M. and Stahl, K.: Modeling drought impact
1052 occurrence based on meteorological drought indices in Europe, *J. Hydrol.*, 530, 37–50,
1053 doi:10.1016/j.jhydrol.2015.09.039, 2015.
- 1054 Stellmes, M., Röder, A., Udelhoven, T. and Hill, J.: Mapping syndromes of land change
1055 in Spain with remote sensing time series, demographic and climatic data, *Land use
1056 policy*, 30(1), 685–702, doi:10.1016/j.landusepol.2012.05.007, 2013.
- 1057 Tucker, C. J.: Red and photographic infrared linear combinations for monitoring
1058 vegetation, *Remote Sens. Environ.*, 8(2), 127–150, doi:10.1016/0034-4257(79)90013-0,
1059 1979.
- 1060 Tucker, C. J., Pinzon, J. E., Brown, M. E., Slayback, D. A., Pak, E. W., Mahoney, R.,
1061 Vermote, E. F. and El Saleous, N.: An extended AVHRR 8-km NDVI dataset
1062 compatible with MODIS and SPOT vegetation NDVI data, *Int. J. Remote Sens.*, 26(20),
1063 4485–4498, doi:10.1080/01431160500168686, 2005.
- 1064 Udelhoven, T., Stellmes, M., del Barrio, G. and Hill, J.: Assessment of rainfall and
1065 NDVI anomalies in Spain (1989-1999) using distributed lag models, *Int. J. Remote
1066 Sens.*, 30(8), 1961–1976, doi:10.1080/01431160802546829, 2009.
- 1067 Vicente-Serrano, S. M.: Spatial and temporal analysis of droughts in the Iberian
1068 Peninsula (1910-2000), *Hydrol. Sci. J.*, 51(1), doi:10.1623/hysj.51.1.83, 2006.
- 1069 Vicente-Serrano, S. M.: Evaluating the impact of drought using remote sensing in a
1070 Mediterranean, Semi-arid Region, *Nat. Hazards*, 40(1), doi:10.1007/s11069-006-0009-
1071 7, 2007.
- 1072 Vicente-Serrano, S. M. and Beguería, S.: Comment on “Candidate distributions for
1073 climatological drought indices (SPI and SPEI)” by James H. Stagge et al., *Int. J.
1074 Climatol.*, 36(4), doi:10.1002/joc.4474, 2016.
- 1075 Vicente-Serrano, S. M., Cuadrat-Prats, J. M. and Romo, A.: Aridity influence on
1076 vegetation patterns in the middle Ebro Valley (Spain): Evaluation by means of AVHRR
1077 images and climate interpolation techniques, *J. Arid Environ.*, 66(2),
1078 doi:10.1016/j.jaridenv.2005.10.021, 2006.
- 1079 Vicente-Serrano, S. M., Beguería, S. and López-Moreno, J. I.: A multiscalar drought
1080 index sensitive to global warming: The standardized precipitation evapotranspiration
1081 index, *J. Clim.*, 23(7), doi:10.1175/2009JCLI2909.1, 2010.
- 1082 Vicente-Serrano, S. M., Beguería, S. and López-Moreno, J. I.: Comment on
1083 Characteristics and trends in various forms of the Palmer Drought Severity Index
1084 (PDSI) during 1900-2008 by Aiguo Dai, *J. Geophys. Res. Atmos.*, 116(19), 2011.
- 1085 Vicente-Serrano, S. M., Beguería, S., Lorenzo-Lacruz, J., Camarero, J. J., López-



- 1086 Moreno, J. I., Azorin-Molina, C., Revuelto, J., Morán-Tejeda, E. and Sanchez-Lorenzo,
1087 A.: Performance of drought indices for ecological, agricultural, and hydrological
1088 applications, *Earth Interact.*, 16(10), doi:10.1175/2012EI000434.1, 2012.
- 1089 Vicente-Serrano, S. M., Gouveia, C., Camarero, J. J., Beguería, S., Trigo, R., López-
1090 Moreno, J. I., Azorin-Molina, C., Pasho, E., Lorenzo-Lacruz, J., Revuelto, J., Morán-
1091 Tejeda, E. and Sanchez-Lorenzo, A.: Response of vegetation to drought time-scales
1092 across global land biomes, *Proc. Natl. Acad. Sci. U. S. A.*, 110(1),
1093 doi:10.1073/pnas.1207068110, 2013.
- 1094 Vicente-Serrano, S. M., Camarero, J. J. and Azorin-Molina, C.: Diverse responses of
1095 forest growth to drought time-scales in the Northern Hemisphere, *Glob. Ecol.*
1096 *Biogeogr.*, 23(9), doi:10.1111/geb.12183, 2014a.
- 1097 Vicente-Serrano, S. M., Lopez-Moreno, J.-I., Beguería, S., Lorenzo-Lacruz, J.,
1098 Sanchez-Lorenzo, A., García-Ruiz, J. M., Azorin-Molina, C., Morán-Tejeda, E.,
1099 Revuelto, J., Trigo, R., Coelho, F. and Espejo, F.: Evidence of increasing drought
1100 severity caused by temperature rise in southern Europe, *Environ. Res. Lett.*, 9(4),
1101 doi:10.1088/1748-9326/9/4/044001, 2014b.
- 1102 Vicente-Serrano, S. M., Azorin-Molina, C., Sanchez-Lorenzo, A., Revuelto, J., López-
1103 Moreno, J. I., González-Hidalgo, J. C., Moran-Tejeda, E. and Espejo, F.: Reference
1104 evapotranspiration variability and trends in Spain, 1961-2011, *Glob. Planet. Change*,
1105 121, doi:10.1016/j.gloplacha.2014.06.005, 2014c.
- 1106 Vicente-Serrano, S. M., Azorin-Molina, C., Sanchez-Lorenzo, A., Revuelto, J., Morán-
1107 Tejeda, E., López-Moreno, J. I. and Espejo, F.: Sensitivity of reference
1108 evapotranspiration to changes in meteorological parameters in Spain (1961-2011),
1109 *Water Resour. Res.*, 50(11), doi:10.1002/2014WR015427, 2014d.
- 1110 Vicente-Serrano, S. M., Cabello, D., Tomás-Burguera, M., Martín-Hernández, N.,
1111 Beguería, S., Azorin-Molina, C. and Kenawy, A. E.: Drought variability and land
1112 degradation in semiarid regions: Assessment using remote sensing data and drought
1113 indices (1982-2011), *Remote Sens.*, 7(4), doi:10.3390/rs70404391, 2015.
- 1114 Vicente-Serrano, S. M., Tomas-Burguera, M., Beguería, S., Reig, F., Latorre, B., Peña-
1115 Gallardo, M., Luna, M. Y., Morata, A. and González-Hidalgo, J. C.: A High Resolution
1116 Dataset of Drought Indices for Spain, *Data*, 2(3), 2017.
- 1117 Vicente-Serrano, S. M., Martín-Hernández, N., Reig, F., Azorin-Molina, C., Zabalza, J.,
1118 Beguería, S., Domínguez-Castro, F., El Kenawy, A., Peña-Gallardo, M., Noguera, I. and
1119 García, M.: Vegetation greening in Spain detected from long term and high spatial
1120 resolution data (1981-2015), *Submitt. to Glob. Planet. Chang.*, 2018.
- 1121 Wan, Z., Wang, P. and Li, X.: Using MODIS Land Surface Temperature and
1122 Normalized Difference Vegetation Index products for monitoring drought in the
1123 southern Great Plains, USA, *Int. J. Remote Sens.*, 25(1), 61–72,
1124 doi:10.1080/0143116031000115328, 2004.
- 1125 Wang, J., Rich, P. M. and Price, K. P.: Temporal responses of NDVI to precipitation
1126 and temperature in the central Great Plains, USA, *Int. J. Remote Sens.*, 24(11), 2345–
1127 2364, doi:10.1080/01431160210154812, 2003.
- 1128 Xulu, S., Peerbhay, K., Gebreslasie, M. and Ismail, R.: Drought influence on forest
1129 plantations in Zululand, South Africa, using MODIS time series and climate data,
1130 *Forests*, 9(9), doi:10.3390/f9090528, 2018.



- 1131 Yang, S., Meng, D., Li, X. and Wu, X.: Multi-scale responses of vegetation changes
1132 relative to the SPEI meteorological drought index in North China in 2001-2014,
1133 Shengtai Xuebao/ Acta Ecol. Sin., 38(3), 1028–1039, doi:10.5846/stxb201611242398,
1134 2018.
- 1135 Zhang, L., Xiao, J., Zhou, Y., Zheng, Y., Li, J. and Xiao, H.: Drought events and their
1136 effects on vegetation productivity in China, Ecosphere, 7(12), doi:10.1002/ecs2.1591,
1137 2016.
- 1138 Zhang, Q., Kong, D., Singh, V. P. and Shi, P.: Response of vegetation to different time-
1139 scales drought across China: Spatiotemporal patterns, causes and implications, Glob.
1140 Planet. Change, 152, 1–11, doi:10.1016/j.gloplacha.2017.02.008, 2017.
- 1141 Zhao, M. and Running, S. W.: Drought-induced reduction in global terrestrial net
1142 primary production from 2000 through 2009, Science (80-.), 329(5994), 940–943,
1143 doi:10.1126/science.1192666, 2010.
- 1144 Zhao, M., Geruo, A., Velicogna, I. and Kimball, J. S.: Satellite observations of regional
1145 drought severity in the continental United States using GRACE-based terrestrial water
1146 storage changes, J. Clim., 30(16), 6297–6308, doi:10.1175/JCLI-D-16-0458.1, 2017.
- 1147 Zhao, X., Wei, H., Liang, S., Zhou, T., He, B., Tang, B. and Wu, D.: Responses of
1148 natural vegetation to different stages of extreme drought during 2009-2010 in
1149 Southwestern China, Remote Sens., 7(10), 14039–14054, doi:10.3390/rs71014039,
1150 2015.
- 1151



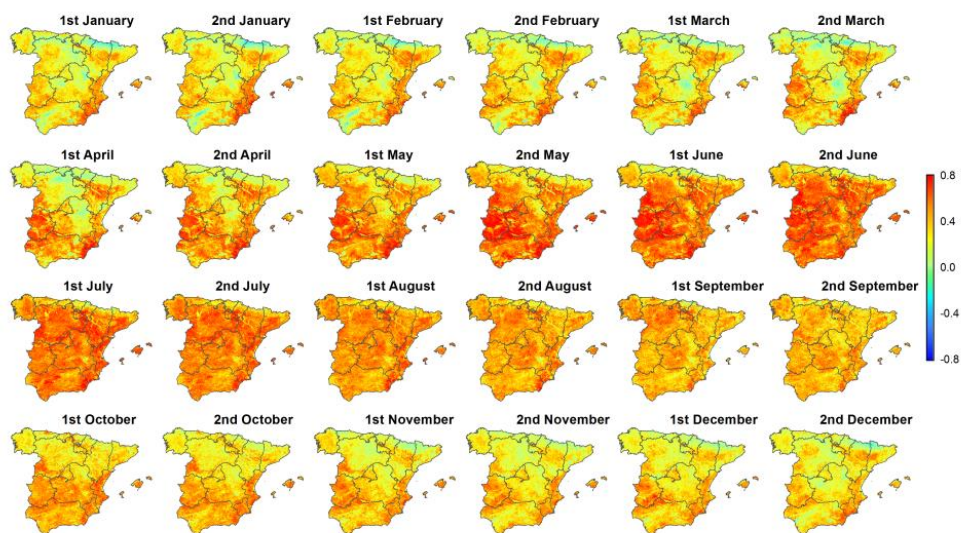
1152

1153

1154

1155

Figure 1: Spatial distribution of the Pearson's r correlation coefficient calculated between the sNDVI and different SPEI time scales for different semi-monthly periods.



1156

1157 Figure 2: Spatial distribution of the maximum correlation between the sNDVI and the
1158 SPEI during the different semi-monthly periods.

1159

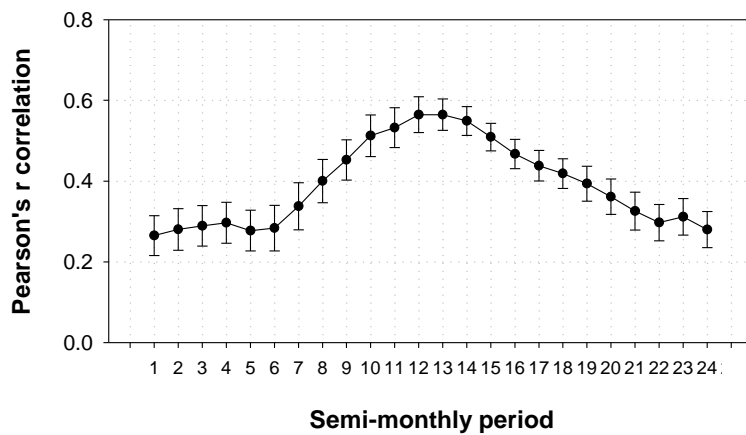


1160 Table 1: Percentage of the total surface area according to the different significance
 1161 categories of Pearson's r correlations between the sNDVI and SPEI.

	Negative ($p < 0.05$)	Negative ($p > 0.05$)	Positive ($p > 0.05$)	Positive ($p < 0.05$)
1st Jan	0.3	9.8	41.3	48.6
2nd Jan	0.4	8.7	40.2	50.7
1st Feb	0.3	7.5	39.9	52.3
2nd Feb	0.1	7.5	39.0	53.4
1st Mar	0.2	8.9	41.6	49.4
2nd Mar	0.2	11.3	38.2	50.3
1st Apr	0.0	7.6	34.9	57.5
2nd Apr	0.0	3.4	27.0	69.7
1st May	0.0	1.6	19.0	79.4
2nd May	0.0	0.9	14.2	84.9
1st Jun	0.0	1.2	10.8	88.0
2nd Jun	0.0	0.5	7.4	92.0
1st Jul	0.0	0.3	5.3	94.4
2nd Jul	0.0	0.1	4.5	95.4
1st Aug	0.0	0.1	5.9	94.1
2nd Aug	0.0	0.2	10.6	89.2
1st Sep	0.0	0.6	14.0	85.4
2nd Sep	0.0	0.4	16.9	82.6
1st Oct	0.0	1.5	24.5	74.0
2nd Oct	0.0	1.9	31.1	67.0
1st Nov	0.0	4.5	35.6	59.8
2nd Nov	0.0	4.8	41.8	53.4
1st Dec	0.0	4.4	38.9	56.7
2nd Dec	0.2	5.9	43.1	50.8

1162

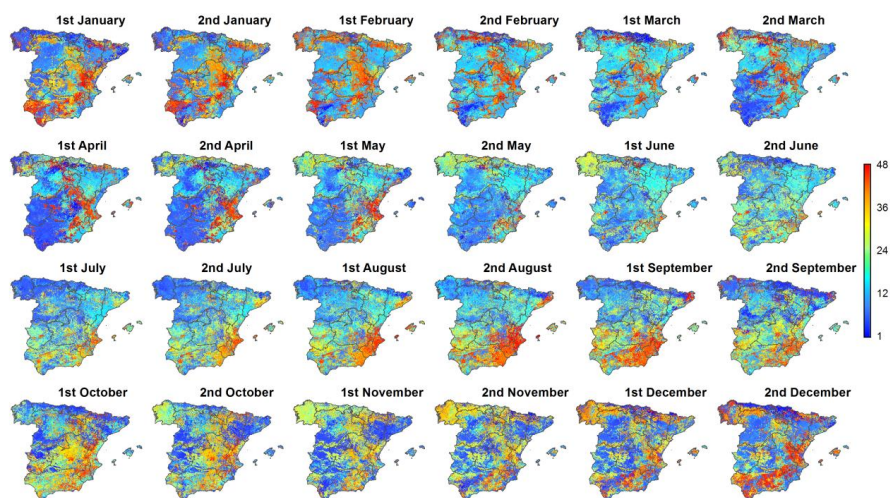
1163



1164

1165 Figure 3: Spatial Average and standard error of the Pearson's r correlation coefficient
1166 between the sNDVI and SPEI time series.

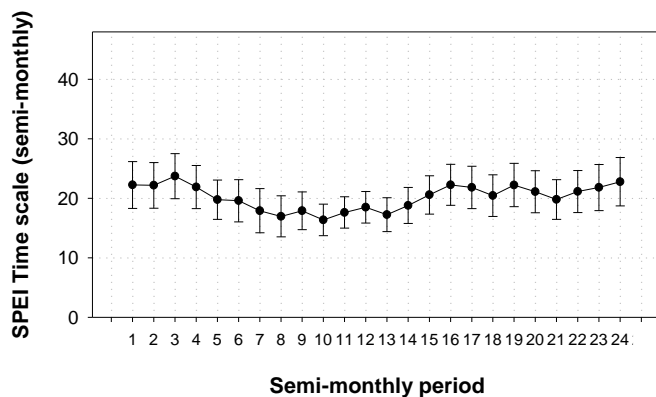
1167



1168

1169 Figure 4: Spatial distribution of the SPEI time scales at which the maximum correlation
1170 between the sNDVI and SPEI is found for each one of the semi-monthly periods.

1171

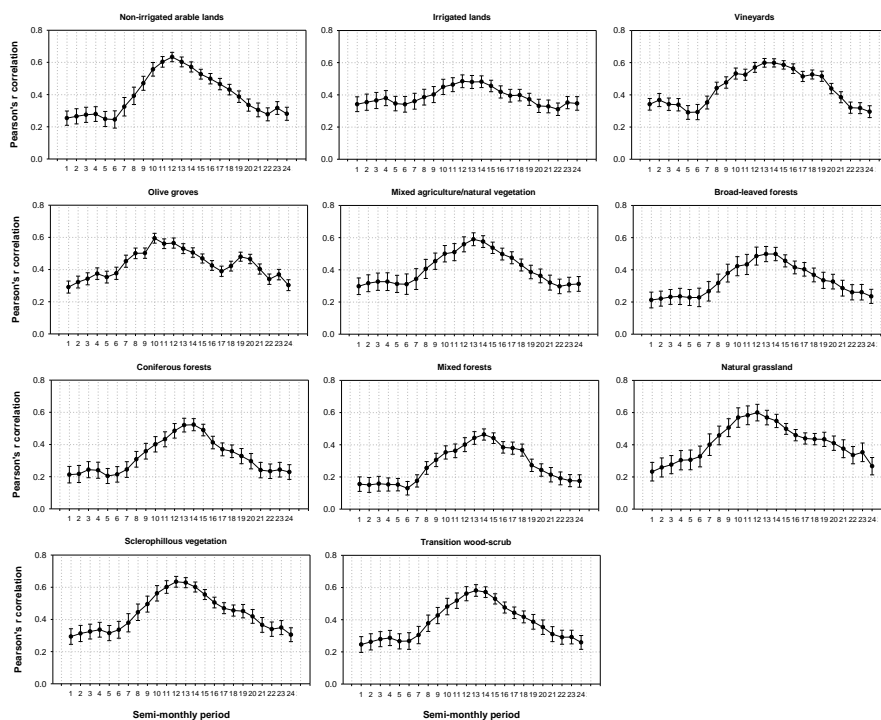


1172

1173 Figure 5: Average and standard error of the SPEI time scale at which the maximum
1174 Pearson's r correlation coefficient between the sNDVI and SPEI is found.

1175

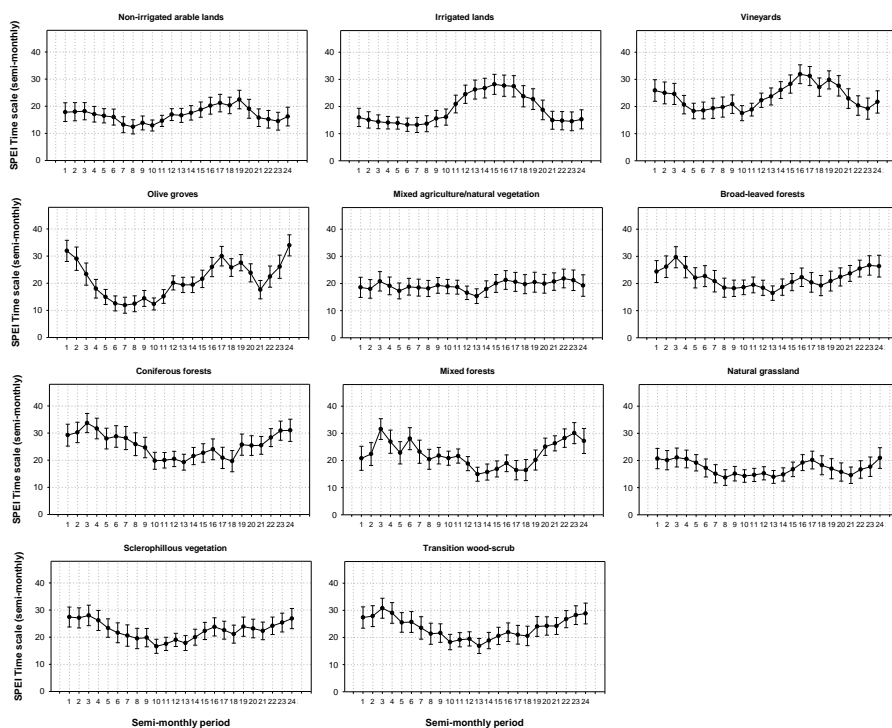
1176



1177

1178 Figure 6: Average and standard error of the Pearson's r correlation coefficient between
1179 the sNDVI and SPEI for the different land cover types.

1180



1181

1182

1183

1184

1185

Figure 7: Average and standard error of the SPEI time scale at which the maximum Pearson's r correlation coefficient was found between the sNDVI and SPEI for the different land cover types.

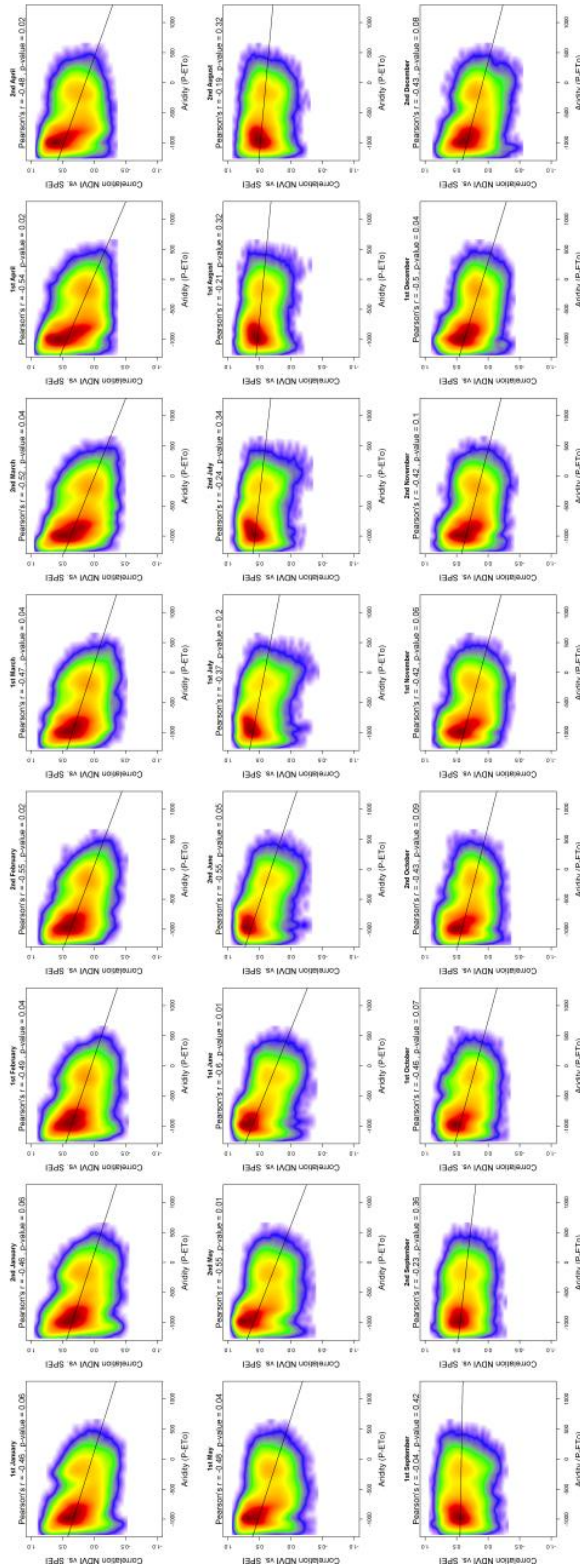


Figure 8. Scatterplots showing the relationships between the maximum correlation obtained between the sNDVI and the SPEI and the climate aridity (Precipitation minus Atmospheric Evaporative Demand). Given the high number of data, the signification of the correlation was obtained by a bootstrap method. 1000 random samples were extracted of 30 data points each, from which correlations and p-values were obtained. The final signification was assessed by means of the average of the obtained correlation coefficients and p-values, which are indicated in the figure.

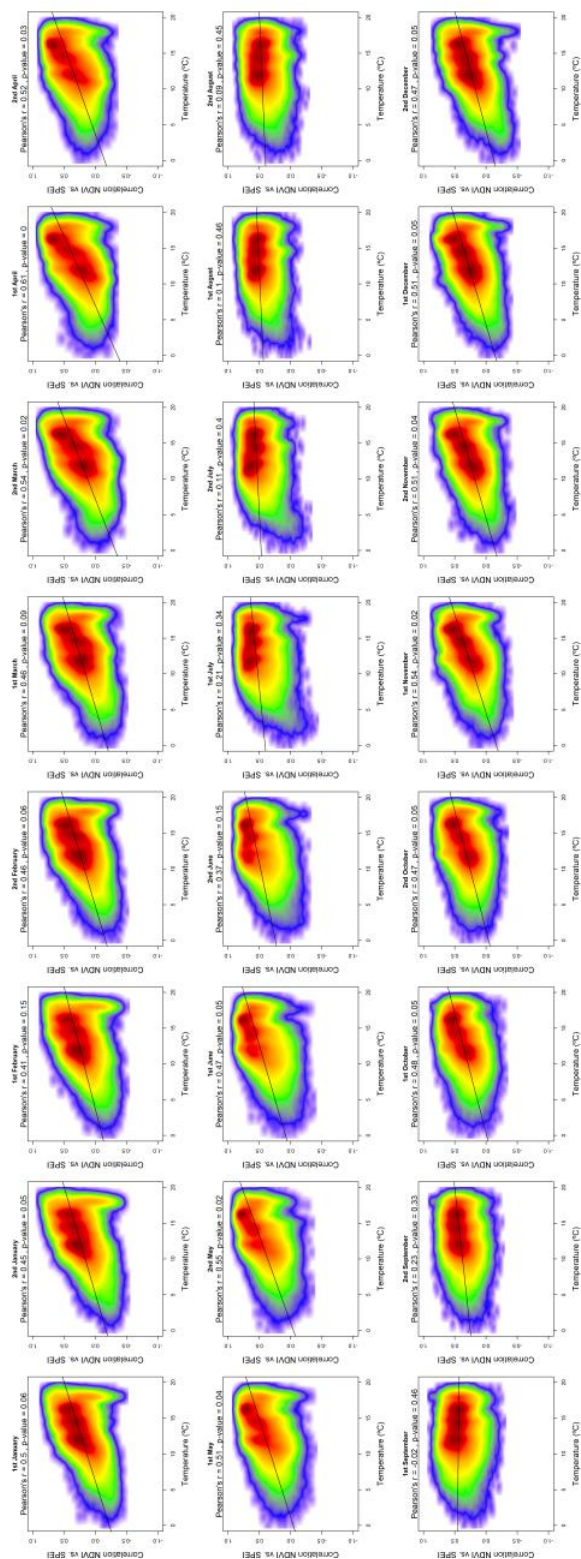


Figure 9. Scatterplots showing the relationships between the maximum correlation obtained between the sNDVI and the SPEI and the average air temperature. Given the high number of points the signification of correlation was obtained by means of 1000 random samples of 30 cases from which correlations and p-values were obtained. The final signification was assessed by means of the average of the obtained p-values.

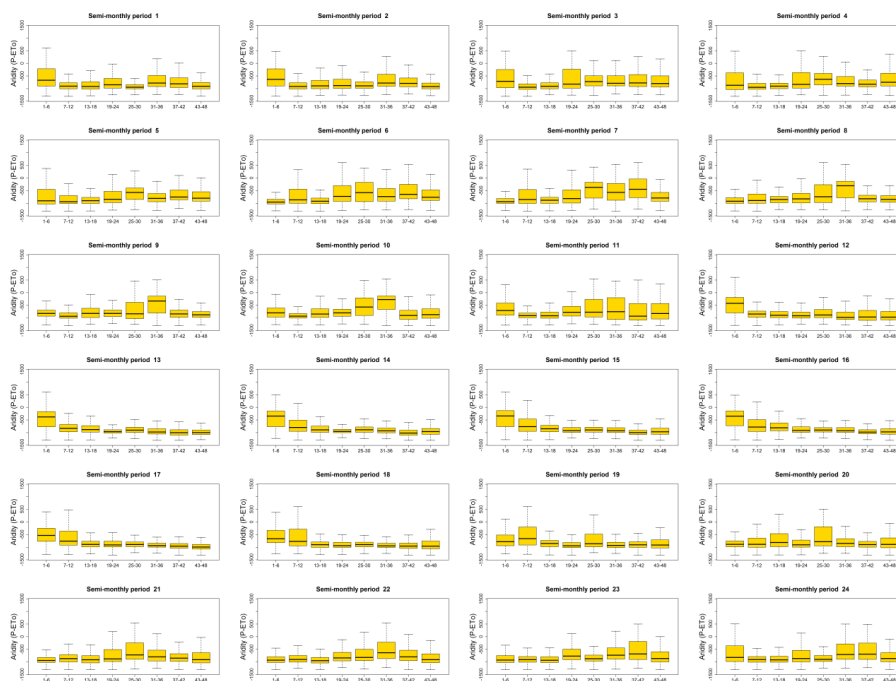


Figure 10: Box plots showing the climate aridity values , as a function of the SPEI time scales at which the maximum correlation between the sNDVI and SPEI is recorded

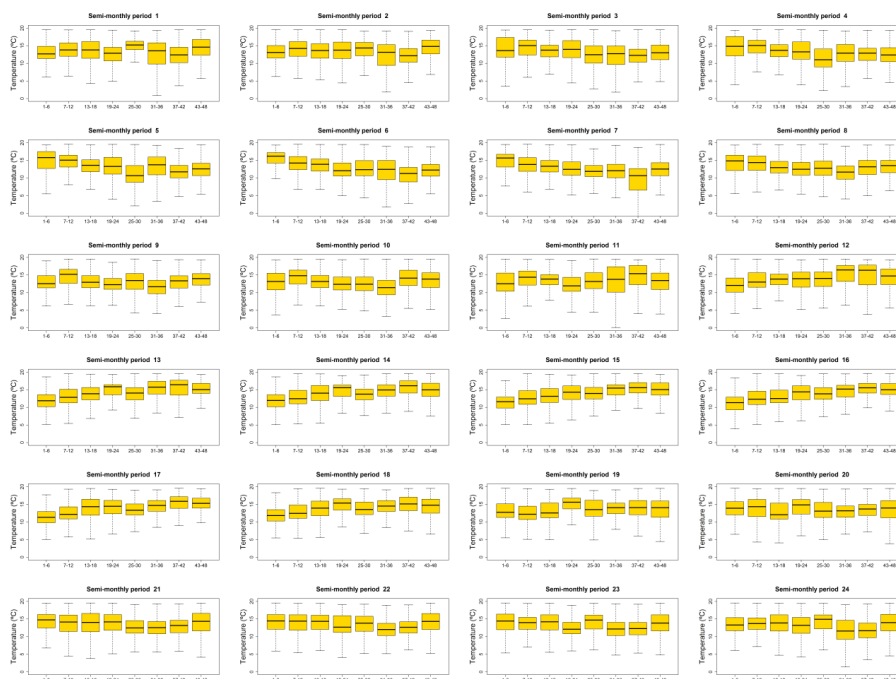


Figure 11: Box plots showing air temperature values, as a function of the SPEI time scales at which the maximum correlation between the sNDVI and SPEI is recorded.

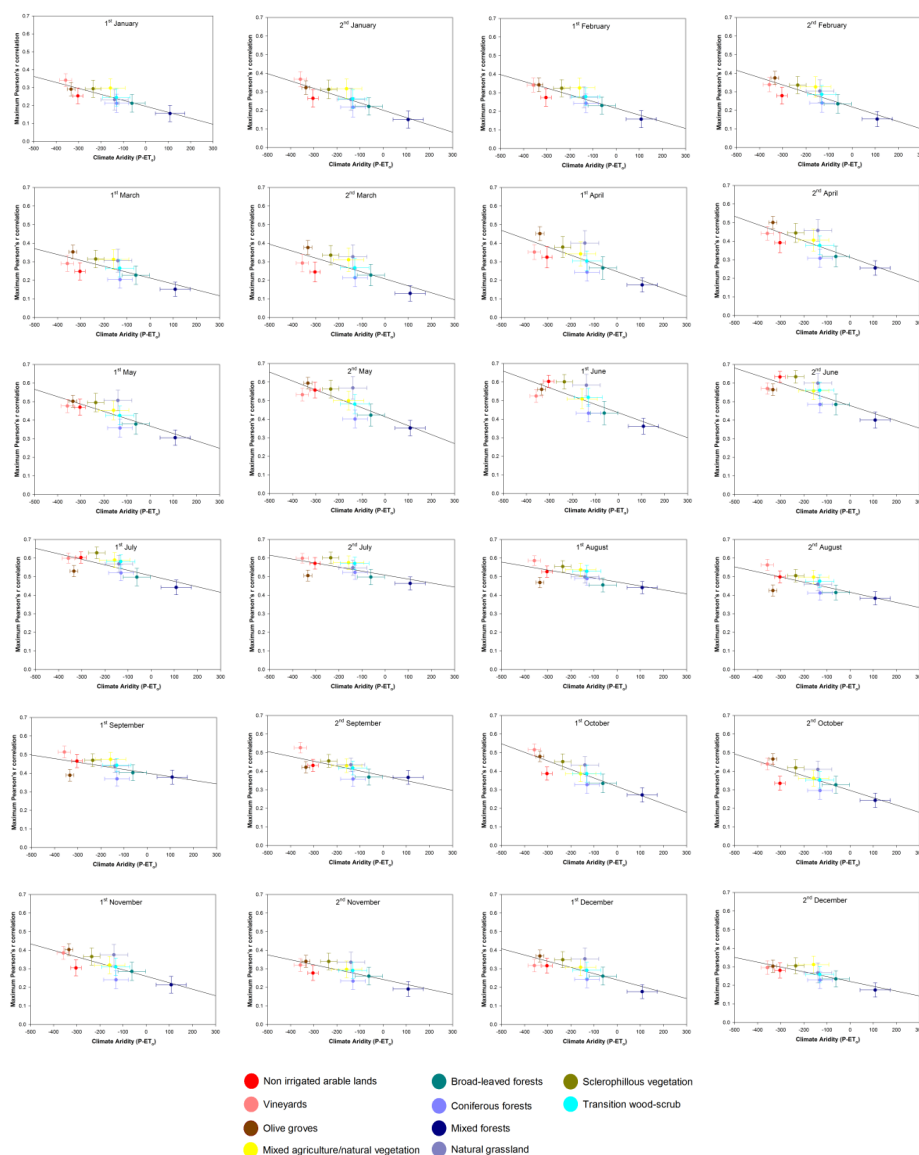


Figure 12: Scatterplots showing the relationship between the mean annual aridity and the maximum correlation found between the sNDVI and the SPEI in the different land cover types analysed in this study. Vertical and horizontal bars represent $\frac{1}{4}$ of standard deviation around the mean values.

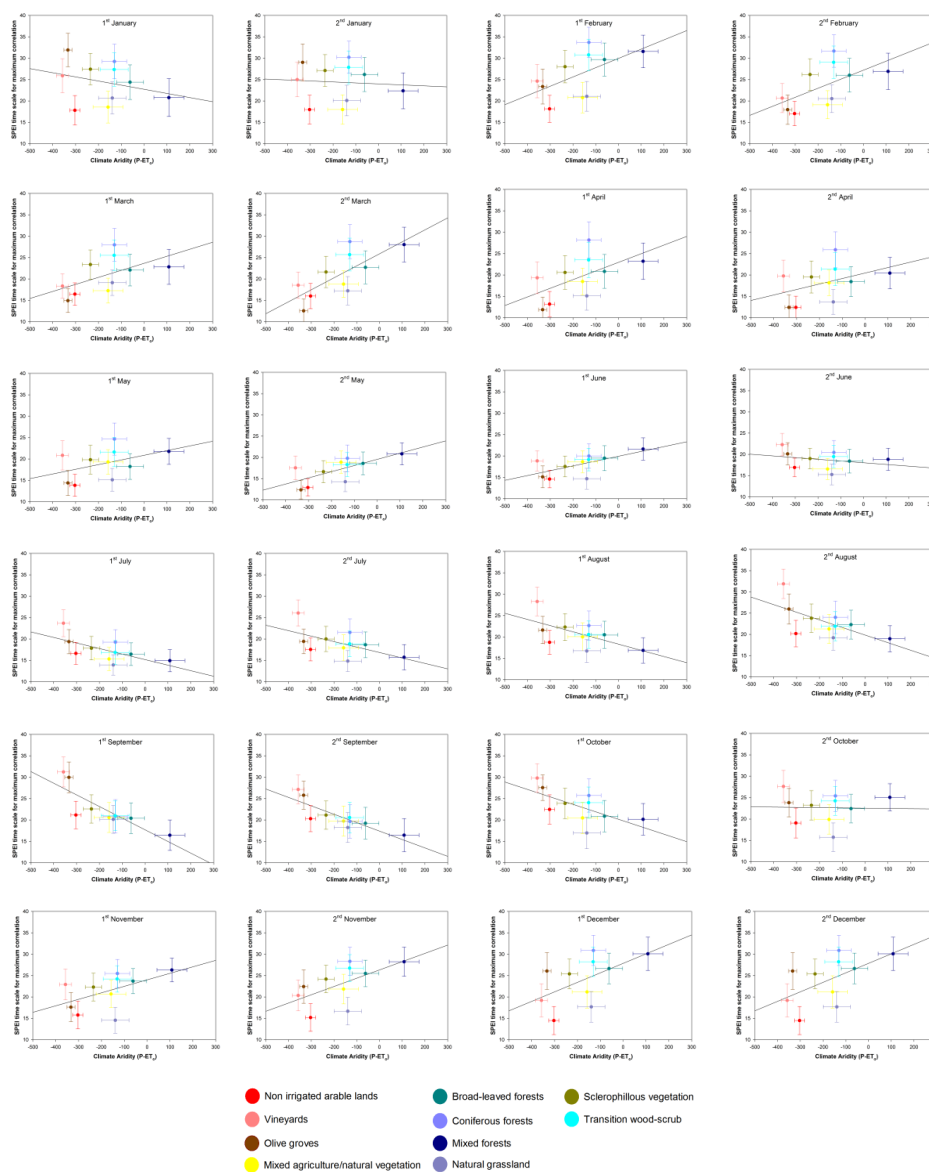


Figure 13: Scatterplots showing the relationship between the mean annual aridity and the SPEI time scale at which the maximum correlation is found between the sNDVI and SPEI for the different land cover types. Vertical and horizontal bars represent $\frac{1}{4}$ of standard deviation around the mean values.